Potential Performance Improvements of Floor Heating Systems in Light-weight Floors

A Numerical Study of HSB Living Lab

Master's Thesis in the Master's Programme Structural Engineering and Building Technology

VICTORIA STIGEMYR HILL

Potential Performance Improvements of Floor Heating Systems in Light-weight Floors

A Numerical Study of HSB Living Lab

Master's Thesis in the Master's Programme Structural Engineering and Building Technology

VICTORIA STIGEMYR HILL

Department of Civil and Environmental Engineering
Division of Building Technology
Building Physics
CHALMERS UNIVERSITY OF TECHNOLOGY
Göteborg, Sweden 2016

Potential Performance Improvements of Floor Heating Systems in Light-weight Floors
A Numerical Study of HSB Living Lab

Master's Thesis in the Master's Programme Structural Engineering and Building Technology

VICTORIA STIGEMYR HILL

Department of Civil and Environmental Engineering
Division of Building Technology
Building Physics
Chalmers University of Technology
SE-412 96 Göteborg
Sweden
Telephone: + 46 (0)31-772 1000

Cover:
Temperature distribution of numerical simulated floor heating system embedded into the floor construction of HSB Living Lab.
Department of Civil and Environmental EngineeringGöteborg, Sweden, 2016

Potential Performance Improvements of Floor Heating Systems in Light-weight Floors

A Numerical Study of HSB Living Lab

Master's thesis in the Master's Programme Structural Engineering and Building Technology

VICTORIA STIGEMYR HILL

Department of Civil and Environmental Engineering
Division of Building Technology
Building Physics
Chalmers University of Technology

ABSTRACT

Floor heating system is a heating system with the ability to both supply small amount of heat and operate on low temperate water, required by low-energy buildings and alternative energy supply systems. Embedded into a floor construction with high thermal inertia, the most energy efficient floor heating system is obtained. While in combination with a light-weight construction, the floor heating system is not as energy efficient.

HSB Living Lab is a steel-framed modular building with student housing and research infrastructure, situated at Chalmers University of Technology, which consist of short- and long-term research projects. Due to the light-weight construction, HSB Living Lab offers possibilities to investigate performance improvements of floor heating systems in light-weight floors by experiments.

The purpose of this study is to develop an in-depth numerical model of a floor heating system. Further, the model is applied to the floor heating system of HSB Living Lab with the aim to investigate theoretical improvements, i.e. energy efficiency and self-regulation ability of floor heating systems embedded into light-weight floor constructions.

The study is performed by simulating the floor construction with the numerical software COMSOL Multiphysics. The in-depth numerical model is based on modules simulating heat transfer in solids and heat transfer in pipes. Three improvements are studied; increased heat distribution from the floor heating system by inserting a heat conductive layer of graphite, increased thermal mass of the floor construction by embed the pipes into screed and a combined investigation of the two improvements.

The study shows declined and insignificantly improved performance of the floor heating system when investigating the increase of thermal mass respectively heat distribution. Further by combining the two improvements, the heat transfer improves and it operates similar as a floor heating system embedded into a floor construction with high thermal inertia.

Key words: HSB Living Lab, Floor heating system, Light-weight floor, Self-regulation ability, COMSOL Multiphysics

Prestanda Förbättringar av Golvvärme Belagt i Lättvikts Golv
En Numerisk Studie om Potentiella Experiment i HSB Living Lab

Examensarbete inom masterprogrammet Structural Engineering and Building Technology

VICTORIA STIGEMYR HILL

Institutionen för bygg- och miljöteknik
Avdelningen för Byggnadsteknologi
Byggnadsfysik
Chalmers tekniska högskola

SAMMANFATTNING

Golvvärme är ett värmesystem med möjlighet att appliceras till lågtempererade system samt tillföra liten mängd värme, vilket krävs av alternativa energisystem samt byggnader med låg energiförbrukning. Det mest energieffektiva golvsystemet erhålls i kombination med en golvkonstruktion med hög termisk tröghet, medan system i en lätt golvkonstruktion inte är lika energieffektiva.

HSB Living Lab är en modulbyggnad med stålstomme placerat på Chalmers Tekniska högskola, som innerhåller kort- respektive långvariga foskningsprojekt. På grund av den lätta konstruktionen, erbjuder HSB Living Lab möjligheter att undersöka prestandaförbättringar av golvvärmesystem i kombination med en lätt golvkonstruktion.

Syftet med studien är att utveckla en fördjupad numerisk model av ett golvvärmesystem. Vidare appliceras modellen på golvvärmesystemet i HSB Living Lab, med ändamålet är att undersöka teoretiska förbättringar av golvvärmesystem i en golvkonstruktion med låg termisk tröghet.

Studien genomförs med numeriska simuleringar i programmet COMSOL Multiphysics. Simuleringen av den fördjupade numeriska modellen, baseras på moduler som beräknar värmeöverförning i solida material samt rörledningar. De tre potentiella förbättringarna som undersöks är; ökad värmefördelning från golvvärmesystemet genom tillsätta ett värmeledande sikt av grafit, ökad termisk tröghet av golvkonstruktionen med rörledningar ingjutna i cement och en kombinerad undersökning av de två potientiella förbättringarna.

Undersökningen visar en minskad samt obetydlig ökning i prestanda av golvvärmesystemet, vid simulering av ökad termisk tröghet respektive värmefördelning. Genom att kombinera förbättringarna, förbättras värmetillförseln från systemet och liknande prestanda som ett golvsystem placerat i trögt golvsystem erhålls.

Nyckelord: HSB Living Lab, Golvvärme, Lätt golvkonstruktion, Självregleringsförmåga, COMSOL Multiphysics

II

Contents

Preface

The Master Thesis studies potential improvements of floor heating systems embedded into light-weight floor construction by a numerical model in COMSOL Multiphysics 5.2. Further, the thesis provides with future possible experiments researched in HSB Living Lab. The work was carried out at the Division of Building Technology, Department of Civil and Environmental Engineering at Chalmers University of Technology in Gothenburg, Sweden.

The examiner and supervisor of the thesis was Angela Sasic Kalagasidis, Division of Building Technology. I want to thank Angela for her guidance, supervision and ability to make time for my questions during the thesis work. I also want to give a special thanks to Henrik Karlsson at SP Technical Research Institute of Sweden, who helped with additional supervision during his parental leave.

Finally, I want to thank Tommie Månsson, Division of Building Technology, who helped with modelling in COMSOL, and for borrowing his computer as well as his time.

Gothenburg May 2016

Victoria Stigemyr Hill

Notations

Roman upper case letters

A	Area	$[\text{m}^2]$
c_p	Specific heat capacity at constant pressure	$[\text{J/kg} \cdot \text{K}]$
c_v	Specific heat capacity at constant volume	$[\text{J/kg} \cdot \text{K}]$
d	Thickness	$[\text{m}]$
d_h	Hydraulic diameter	$[\text{m}]$
$F_{1,2}$	View factor between two surfaces	$[-]$
f_D	Darcy friction factor	$[-]$
h	Heat transfer coefficient	$[\text{W/m}^2 \cdot \text{K}]$
I_{sol}^0	Direct solar radiation	$[\text{W/m}^2]$
K	Thermal conductance	$[\text{W/K}]$
k	Thermal conductivity in COMSOL Multiphysics	$[\text{W/m} \cdot \text{K}]$
L	Length	$[\text{m}]$
l	Length	$[\text{m}]$
Q	-Heat flow rate	$[\text{W}]$
$Q_{1,2}$	-Heat flow rate between two surfaces	$[\text{W}]$
q	Heat flux	$[\text{W/m}^2]$
R	Thermal resistance	$[\text{K/W}]$
r	Radius	$[\text{m}]$
T	Temperature	$[\text{K}]$
$T_{1,2}$	Temperature between two surfaces	$[\text{K}]$
t	Time	$[\text{s}]$
t_c	Time constant	$[\text{s}]$
U	Overall thermal transmittance	$[\text{W/m}^2\text{K}]$
u	Velocity	$[\text{m/s}]$
V	Volumetric flow rate	$[\text{m}^3/\text{s}]$
Z	Wall perimeter	$[\text{m}]$

Greek case letters

α	Heat transfer coefficient	$[\text{W/m}^2\text{K}]$
α_{sol}	Solar radiation absorptivity	$[\text{W/m}^2\text{K}]$
η	Insulation efficiency	$[-]$
ϵ	Emissivity	$[-]$

λ	Thermal conductivity	$[\text{W/m} \cdot \text{K}]$
ρ	Density	$[\text{kg/m}^3]$
γ	Heat flux	$[\text{W/mK}]$
θ	Angle of incidence	$[-]$
σ	Stefan-Boltzmann constant	$[\text{W/m}^2\text{K}^4]$

Subscripts

a	Air
c	Convection
cd	Conduction
e	Exterior
eq	Equivalent
f	Fluid
i	Interior
r	Radiation
s	Surface
se	Exterior surface
si	Interior surface
1	Surface one
2	Surface two

1   Introduction

Development of low energy buildings and alternative energy supply systems, such as sun energy and waste heat, is increasing due to large proportion of energy consumed in the construction sector. Furthermore, improvements of building heating systems are necessary to obtain satisfying indoor climate and efficient heat release. The improvements require low temperate systems with water as medium, to operate with the alternative energy supply systems. At the same time, the heat decreases by the well-insulated buildings.

A heating system with variation ability is floor heating, which embedded into the floor construction operates on both electricity and a heated medium. In combination with well-insulated buildings, floor heating systems functions on low temperatures, essential for the utilization of alternative energy supply systems. When floor heating systems are combined with heavy-weight floor, such as concrete, better abilities to store energy are obtained, compared with an arrangement with light-weight floor (Karlsson, 2010). The explanation is due to the high thermal inertia of the heavy-weight floor.

HSB Living Lab is a modular building that consists of short- and long-term research projects. The building will be relocated after the project time of ten years, therefore the entire building is steel-framed and light-weight. Two of the four floors in the building have a water-based floor heating system installed, with the intention to improve floor heating systems in light-weight floors by experiments.

This Master Thesis consists of investigating theoretical improvements of floor heating systems embedded into light-weight floor constructions by a numerical model. The numerical model is applied to the floor heating system in HSB Living Lab, as a case study, where future experiments of investigated improvements will be researched. The major design challenges of floor heating systems embedded into light-weight floors are heat distribution from the heated medium to wanted area and the heat resistance of the material surrounding the heated medium. Therefore, the numerical investigation focuses on improving these challenges.

1.1   Aim

The purpose of this study is to develop an in-depth numerical model of a floor heating system. Further, the model is applied to the floor heating system of HSB Living Lab with the aim to investigate potential improvements of floor heating systems embedded into light-weight floor constructions.

The study answers the following questions:

- Which theoretical improvements of light-weight floors are interesting to investigate with the purpose to obtain similar performance as heavy-weight floors?
- What influences do these improvements have on the performance of the floor heating systems, in particular its self-regulation capability?

Depending on the numerical results, which improvements are interesting with regard to future experiments in HSB Living Lab?

1.2   Limitations

The study should by an in-depth numerical model evaluate potential improvements of floor heating systems embedded into light-weight floor constructions. The evaluation is investigating the heat transfer and self-regulation ability of the construction; hence no thoughts are given to supplementary aspects such as economic and environment.

The focus of the study is water based floor heating systems; other systems are mentioned but not considered. Further for the case study of HSB Living Lab, the designed values calculated by consultants are used when assigning boundary conditions. A comparison of simulated result and designed results are not included, due to no information about the design process.

1.3   Method

The in-depth numerical model was developed in the software COMSOL Multiphysics version 5.2. Initially, information about how to simulate floor heating in the software was investigated. From gathered information, the physical modules Heat Transfer in Solids and Heat Transfer in Pipes were chosen to represent the floor heating system. By the Heat Transfer in Pipes module, advanced and time consuming models with CFD simulations was avoided.

In order to verify the in-depth numerical model, a reference model with standard light-weight floor construction solution was created. A comparison between the reference model and a semi-analytical calculation method of floor heating systems, aimed to verify possible dissimilarities. Furthermore, the verification improved understanding of the physical modules in COMSOL Multiphysics.

The case study of HSB Living Lab continued with the verified in-depth numerical model. To evaluate potential improvements of the floor heating system, a Case Study model with design values of the floor heating system in HSB Living Lab was studied. As mentioned earlier, the design values, obtained by consultants, was inserted as boundary conditions but not evaluated with modelled results.

The potential improvements were gathered and established through literature study, knowledge about thermal inertia and heat transfer, and by discussion with professional designers of floor heating systems. In order to collect information about investigations, supplementary interviews were performed. The results of the investigations were analyzed and evaluated with regard to heat transfer and self-regulation ability of the floor heating system, as mentioned above. Further, the study provided conclusion of investigated result and comments on future investigations.

Continuously through the study, general and in-depth information about heat transfer mechanisms, floor heating systems and COMSOL Multiphysics was gathered. With the collected knowledge, physical processes included in the in-

depth numerical model were understood and further improvements of the model were done.

2 Theoretical bases of heat transfer in floor heating systems

Heat that moves into a building might occur due to heat transfer through the building envelope, intentional air movements by ventilation, unintentional air movements by air leakages or heat gained by solar radiation through windows. The heat transfer mechanisms through the building envelope are affected by the building constructions with chosen building materials. The building materials affects both the construction's U-value and how the building manages temperature variations, by its thermal inertia. When the mechanisms are reversed, and heat is moving from the building, additional heat is supplied by a heating system.

Building physics theory, such as energy and mass conservation and heat transfer, are described in the following sections. Continued with presentation of thermal inertia and how this can be taken as an advantage in building constructions.

2.1 Energy conservation

By physical laws, the conservation of thermal energy within a volume states that the difference between the energy that enters and leaves the volume equals the energy that is stored inside the affecting volume. Some heat is stored inside the volume, by the material, called net inflow of heat, q, (Hagentoft, 2001). Heat stored in the volume, is expressed by the density of the material, ρ, specific heat capacity, c, and temperature difference over time according to equation (2.1).

$$-\nabla \boldsymbol{q} = \frac{\partial}{\partial t}(\rho c T) \ [\text{W/m}^3] \tag{2.1}$$

2.2 Heat transfer

Heat transfer is transfer of thermal energy between solid, liquid and gaseous components due to temperature differences (Hagentoft, 2001). There are three different mechanisms of heat transfer; conduction, convection and radiation, and each of them is described in the following sections.

2.2.1 Conduction

Conduction is due to temperature differences, when heat is transported from a higher to a lower temperature (Hagentoft, 2001). By the law of Fourier, conduction through a homogenous and isotropic material is calculated according to equation (2.2).

$$\boldsymbol{q}_{cd} = -\lambda \nabla T \ [\text{W/m}^3] \tag{2.2}$$

2.2.2 Convection

Convection occurs due to the movement of fluids moving, and is either caused naturally by differences in weight due to temperature differences, called natural

convection, or by a driving force (wind, fan, pump), called forced convection (Hagentoft, 2001). The convective heat flow is proportional to the convective heat transfer coefficient, α_c, calculated according to equation (2.3), and a temperature difference. The convective heat transfer coefficient, α_c, depends on natural or forced convection.

$$q_c = \alpha_c(T_s - T_a) \; [\text{W/m}^2] \tag{2.3}$$

2.2.3 Radiation

Radiation occurs due to electromagnetic waves from a body, when it reaches another body a part of the radiation is reflected, absorbed or transmitted into the body (Hagentoft, 2001). In building physics, two types of radiation are distinguished: short wave and long wave radiation.

Short wave radiation is radiation that is visible, such as solar radiation (Hagentoft, 2001). According to Hagentoft (2001), short wave radiation constitutes normally a heat source that can be absorbed or transmitted through a material, i.e. glass. The absorbed part of solar radiation is found as a product between the solar radiation absorptivity, α_{sol}, the direct solar radiation, I_{sol}^0, and the angle of incidence θ, according to equation (2.4).

$$q_r = \alpha_{sol} \cdot I_{sol}^0 \cdot \cos \theta \; [\text{W/m}^2] \tag{2.4}$$

Long wave radiation is invisible for humans, but generates heat from one surface to another. The temperature and emissivity of the surface decides how much radiation that is emitted[2]. The thermal radiation between two surfaces is found as a product between the radiant surface heat transfer coefficient, α_r, expressed in equation (2.5), the area of surface one, A_1, and the temperature difference between the surfaces according to equation (2.6).

$$\alpha_r = \frac{4\sigma \bar{T}_{1,2}^3}{\frac{1-\epsilon_1}{\epsilon_1} + \frac{1}{F_{12}} + \frac{1-\epsilon_2}{\epsilon_2}\frac{A_1}{A_2}} \; [\text{W/m}^2\text{K}] \tag{2.5}$$

$$Q_{12} = \alpha_r \cdot A_1 \cdot (T_1 - T_2) \; [\text{W}] \tag{2.6}$$

2.3 Derived values

The heat transfer mechanisms described above can be calculated by an overall thermal transmittance called U-value, according to equation (2.7).

$$U = \frac{1}{R_{se} + \sum_{i=1}^{N} R_i + R_{si}} \; [\text{W/m}^2\text{K}] \tag{2.7}$$

Where R_{se} and R_{si}, are combined surface resistances due to convection and long-wave radiation, which have standard values of 0.04 and 0.13 W/m²K (Hagentoft, 2001). Further, the total heat transfer is calculated according to equation (2.8).

$$Q = AU(T_i - T_e) \tag{2.8}$$

The total heat transfer might also calculated according to (2.9) by using the thermal conductance, K, or thermal resistance, R, expressed in equation (2.10).

$$Q = K\Delta T = \frac{\Delta T}{R} \text{ [W]} \tag{2.9}$$

$$K = \frac{\lambda}{d} \text{ [W/K]} \quad R = \frac{d}{\lambda} \text{ [K/W]} \tag{2.10}$$

2.4   Thermal inertia

A building's ability to adjust to variations in outdoor climate is known as thermal inertia and the time it takes for the building to adjust is called time delay[1]. The thermal inertia depends on the building materials, if they are heavy-weight, such concrete and brick, or light-weight, such as timber or steel. Heavy-weight materials have often higher specific heat capacity than light-weight materials, hence they have more capability to store heat resulting in a large thermal inertia (Holladay, 2013)

To obtain benefits by thermal inertia, the climate and how it varies needs to be taken into account. For example, a building with low thermal inertia, when rapid heating and cooling is needed, is profitable due to the short time delay[1]. A typical climate with this construction is northern parts, for example Sweden, hence a lot of buildings consist of wood or steel structures. In other parts with high variations of outdoor temperatures, it is advantageous to keep the indoor temperature steady by using the benefits of a large thermal inertia[1].

---

[1] Angela Sasic Kalagasidis (Professor, Civil and Environmental Engineering, Building Technology) lecture in Building Physics Advanced March 30th 2015

3 Floor heating system

Floor heating system is a heating system that is integrated into the floor construction. In comparison with other heating systems, such as radiators, floor heating system has larger heating area thus lower inlet temperatures can be used (Boverket, 2002). The floor heating system operates on electricity or a heated medium embedded as wires respectively pipes into the floor structure. In this section, a simple analytical calculation method of floor heating systems developed by Henrik Karlsson, Researcher at SP Technical Research Institute of Sweden, is presented and discussed. The method provides results of the insulation efficiency of the floor, heat supply to the floor heating system and its inlet water temperature.

3.1 Water based floor heating systems

Water based floor heating system is floor heating systems that operates on water as a heated medium. The system can be installed in different ways, depending on the floor construction, see Figure 3.1. In combination of a concrete slab, the water pipe is embedded into the structure. Due to the high thermal mass of the floor construction, mainly the concrete slab, a uniform heat distribution on the floor surface is obtained. Further, a high time delay, as mentioned in Section 2.3, is achieved because of the high thermal inertia. Thereby, the system adapts slowly to variations in outdoor temperature, especially during spring and autumn, which might result in discomfort indoors (Boverket, 2002). According to the National Board for Housing and Planning, called Boverket (2002), the discomfort is solved by in advance regulation if the heat supply to the floor heating system, either by increasing the water velocity of inlet temperature.
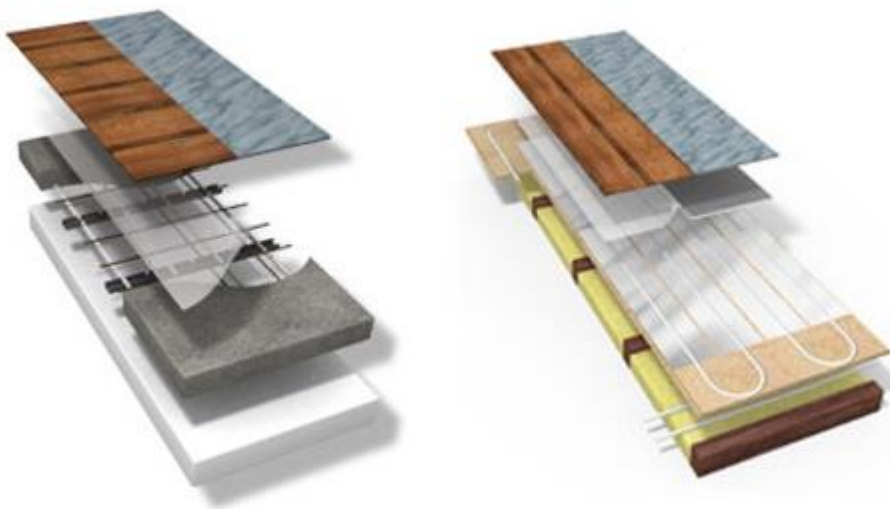

Figure 3.1 Floor heating system installed in heavy-weight floor construction, left picture, and light-weight floor construction, right picture. [Electronic image]
http://www.lksystems.se/sv/LK-Systems-Sverige1/Golvvarme/ [Accessed 2016-06-20]

In light weight floors, such as framed constructions, a uniform heat distribution is harder to obtain due to less energy storage capacity and larger thermal

resistance of the materials that surround the pipes. To improve the heat distribution, plates of a high conductive material, such as aluminum plates, is placed into the floor construction close to the heating medium (Boverket, 2002). Compared with heavy weight floors, the light weight floors adjusts faster to outdoor temperature variations.

The main heat transfer mechanisms from the floor heating systems to the indoor environment are convection and radiation, where 2/3 is caused by radiation[2]. By diagrams, the convective and radiative heat transfer coefficients is decided, see Figure 3.2 and Figure 3.3. A temperature demand on the floor surface is to not exceed a temperature higher than 27 ^{o}C.
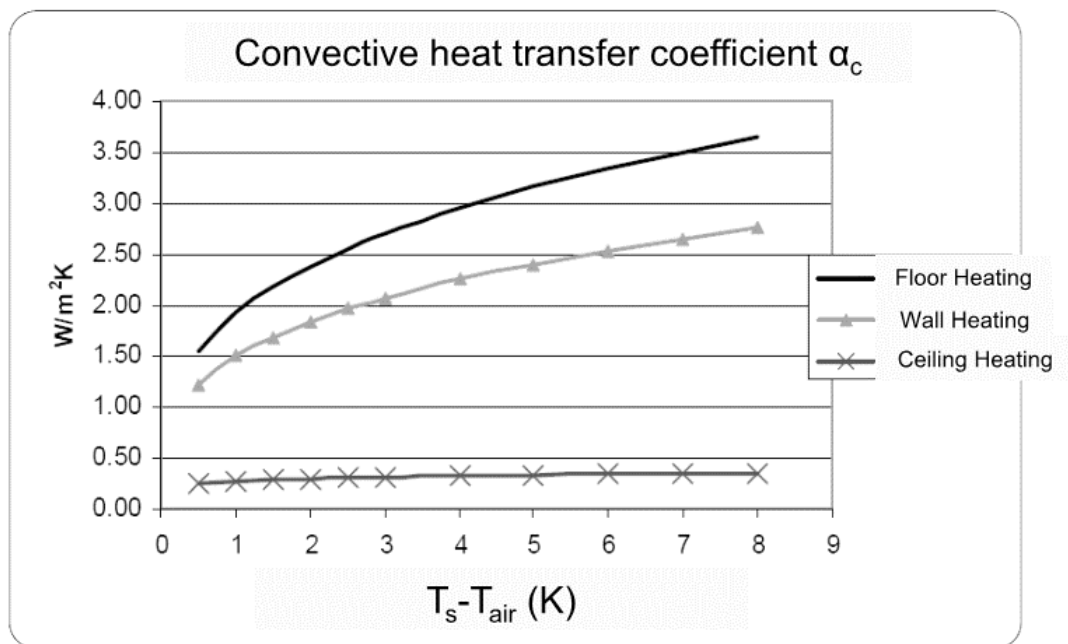

Figure 3.2 Convective heat transfer coefficient between floor surface and ambient air when using a building integrated heating system.
Karlsson, H., (2015). *Convective heat transfer coefficient.* [Picture] Lecture in Building Physics Advanced April 29th 2015, Chalmers University of Technology.

---

[2] Henrik Karlsson (Researcher, SP Technical Research Institute of Sweden) lecture in Building Physics Advanced April 29th 2015
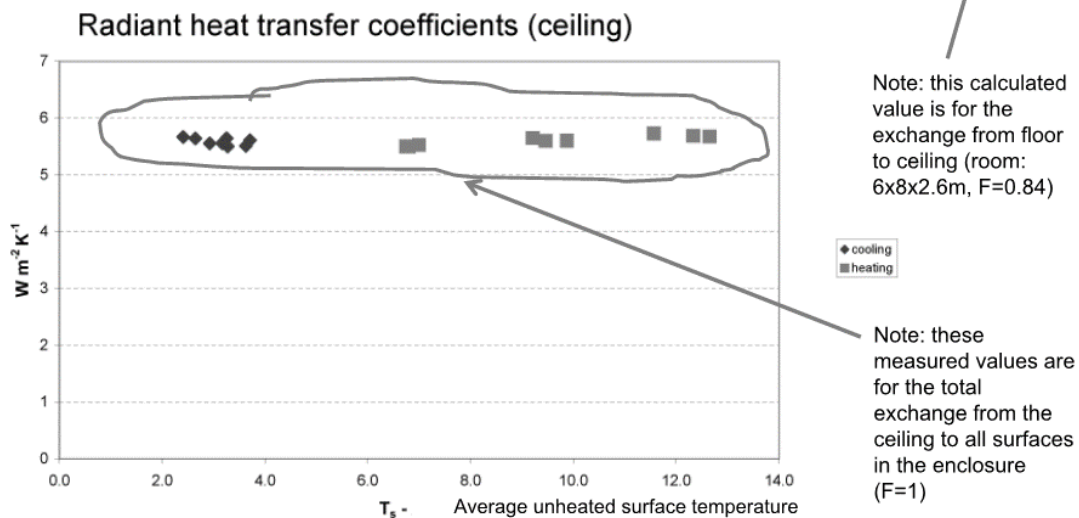
Figure 3.3 Radiant heat transfer coefficient between floor surface and ambient air when using a building integrated heating system
Karlsson, H., (2015). *Radiant heat transfer coefficients (ceiling)*. [Picture] Lecture in Building Physics Advanced April 29th 2015, Chalmers University of Technology.

3.2 Semi-analytical calculation method

The calculation method consist of calculating the insulation efficiency, η, of the floor construction to establish the required heat supply, Q_{supply}, inserted into the floor heating system. With a building integrated heating system, heat is transferred to undesirable parts of the building, for example room or soil below the construction, see Figure 3.4. Thereby the heat supply to the floor heating system is not equal to the heat demand. The insulation efficiency indicates how well insulated the floor construction is, which shows the proportion of heat transferred to the heated area[3]. According to Karlssson[5], a very well insulated floor has an insulation efficiency of $\eta \approx 0.98$ and a inadequately insulated floor an insulation efficiency of $\eta \approx 0.85$.

---

[3] Henrik Karlsson (Researcher, SP Technical Research Institute of Sweden) lecture in Building Physics Advanced April 29th 2015
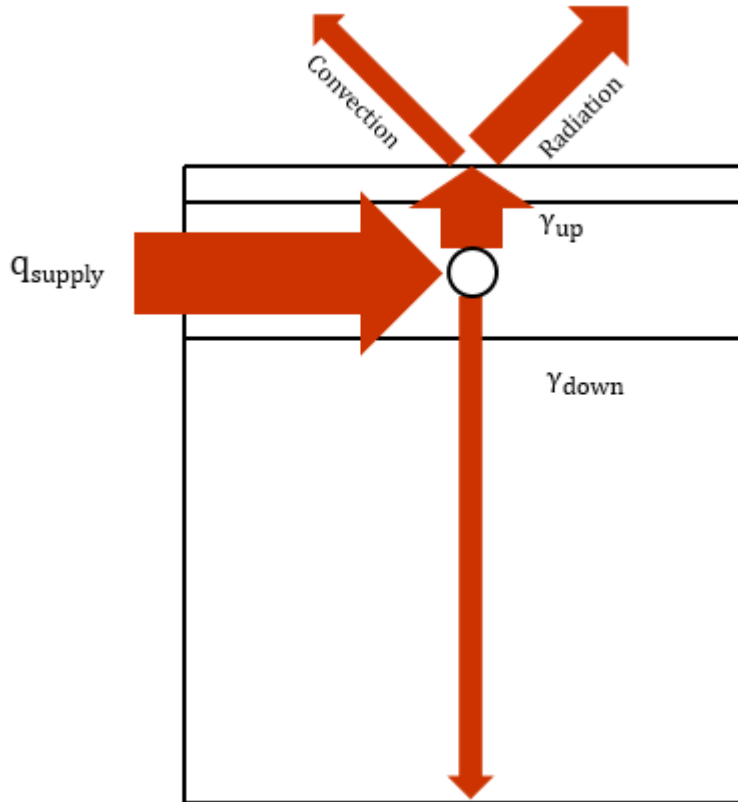
Figure 3.4 Heat transfer mechanisms of a floor heating system

The insulation efficiency and heat supply is calculated according to equations (3.1) respectively (3.2). An alternative to calculate the supplied heat is to determine the heat loss along the water circuit, according to equation (3.3).

$$\eta = \frac{\gamma_{up}}{\gamma_{up} - \gamma_{down}} \ [-] \tag{3.1}$$

$$Q_{supply} = \frac{Q_{demand}}{\eta} \ [W] \tag{3.2}$$

$$Q_{supply} = V_f \rho_f c_{p,f} \Delta T_f \ [W] \tag{3.3}$$

The heat fluxes γ_up and γ_down indicates how well the material transfer heat in the cross section, see Figure 3.4. The upward and downward heat flux is calculated according to equations (3.4) and (3.5).

$$\gamma_{up} = \frac{q_{up}}{T_f - T_i} \ [W/mK] \tag{3.4}$$

$$\gamma_{down} = \frac{q_{down}}{T_f - T_e} \ [W/mK] \tag{3.5}$$

To calculate the upward and downward heat flux, a 2D model can be established in the software COMSOL Multiphysics. The model is simulated with inlet water

temperature of $T_f = 1\ ^\circ\text{C}$ and surrounding temperature of $T_e = 0\,^\circ\text{C}$, to obtain a denominator of 1 $^\circ$C. The upward and downward heat flux rate across the pipe length is found by simulating the 2D transfer through a floor section, similar to Figure 3.4, and integrating the heat flows at the top and bottom boundaries. Further, the simulation results is inserted into equation (3.3) and (3.4) to calculate the upward and downward heat flux.

Furthermore the calculation method consists of calculating the inlet water temperature according to equation (3.6). The inlet water temperature is calculated by a reference temperature, expressed in equation (3.7), which is added to an over-temperature, the second term in equation (3.6).

$$T_f(x = 0) = T_0 + \frac{Q_{demand}}{\eta \cdot K_{eq}} \quad [^\circ\text{C}] \tag{3.6}$$

$$T_0 = T_i \cdot \eta + T_e(1 - \eta) \quad [^\circ\text{C}] \tag{3.7}$$

Where the equivalent conductance, K_{eq}, and characteristic length, l_c, is calculated according to equation (3.8) and (3.9).

$$K_{eq} = V_f \rho c_p \left(1 - e^{\frac{-L_{circuit}}{l_{circuit}}} \right) \quad [\text{W/}^\circ\text{C}] \tag{3.8}$$

$$l_c = \frac{\rho c_p V_f}{\gamma_{up} + \gamma_{down}} \quad [\text{m}] \tag{3.9}$$

3.3 Self-regulation ability of water based floor heating systems

Self-regulation ability is the capability of the floor heating system to regulate the heat supply to the room when disturbances occur (Karlsson, 2008). Basic principle of self-regulation is illustrated in Figure 3.5. The upward heat flux from the floor heating system is designed to match the heat losses from the building, Q, at certain indoor and outdoor conditions. Specifically, the upward heat flux is proportional to the temperature difference between water, in the water circuit, and indoor air, also expressed in equation 3.4. At self-regulation, the water flow rate and inlet water temperature, $T_{f,in}$, are kept constant.
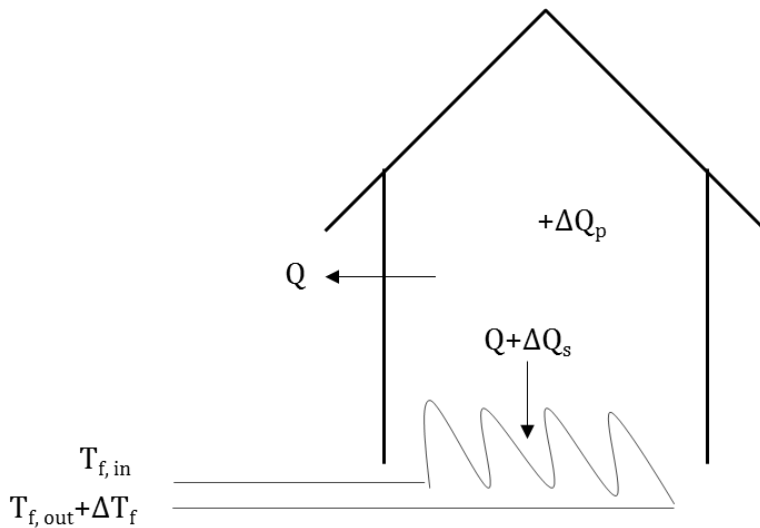
Figure 3.5 Function of self-regulation ability of floor heating systems

When a positive disturbance occurs indoors, i.e. a heat gain $+\Delta Q_p$, the indoor temperature increases. Automatically, the difference between the indoor temperature and the floor surface temperature decreases and less heat is transferred from the floor heating system. As a result, the excess heat appears in the water circuit $+\Delta Q_s$ and the outlet temperature increases, $T_{f,out} + \Delta T_f$, due to less temperature decrease along the pipe. According to Hagentoft and Karlsson (2011), the heat transfer stops when the indoor temperature reaches the inlet temperature, due to high heat gains. The opposite procedure happens when a negative disturbance, a heat loss occurs indoors.

The best self-regulation ability occurs with a low temperature difference between floor surface and indoor temperature, creating the highest utilisation of self-regulated floor heating systems (Karlsson, 2s008).

4   In-depth numerical model

The numerical model of the floor heating system is constructed by using the software COMSOL Multiphysics. Reliable results from the numerical model are obtained by creating a reference model and verifying its result with the calculation method described above in Section 3.2. The reference model demonstrates an invented room, called standard room, where constructions consists of standard solutions such as floor and wall constructions in timber.

In the following sections information about the software COMSOL Multiphysics, standard room and reference model are presented and analysed.

4.1   COMSOL Multiphysics 5.2

COMSOL Multiphysics version 5.2 is the software used to simulate the floor structure. The software models and simulates physical problems with advanced numerical methods (COMSOL, 2016). The physics used are chosen by modules, which is combined to create multi-physics phenomenon.

The software's workspace consists of a Model Builder with a model tree where all data and settings to the model can be assigned, see Figure 4.1. In the model tree model studies are calculated and requested results is obtained. In the graphics window created geometries are shown which helps to assign material as well as boundary conditions depending on the physic module.
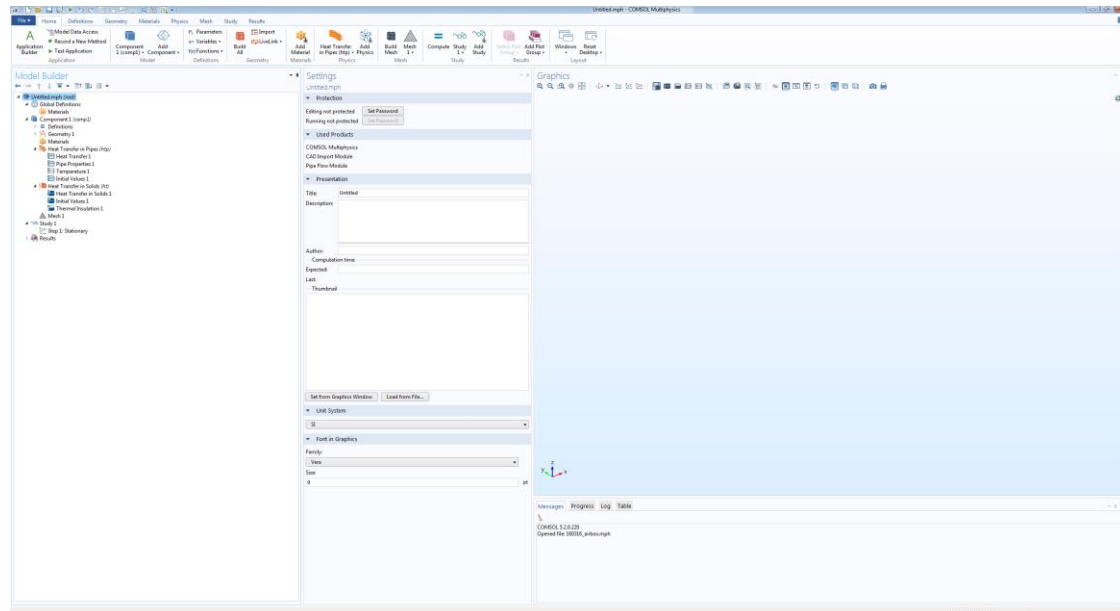

Figure 4.1 Workspace in COMSOL Multiphysics 5.2

4.2   Standard room

The invented standard room, consisting of constructions by standard solutions, is assumed to be placed in the middle of a building with only one external wall. Therefore this intermediate floor construction acts both as a floor and an internal roof. The building, with the standard room, is placed in outdoor conditions applicable for Gothenburg in Sweden.

The geometry of the standard room is 3.045*3.045*2.912 m, which is decided by the centre distance between the studs in the standard solutions of wall and floor constructions. A light-weight construction is chosen, consisting of wooden beams and studs. More information about the wall construction is found in Appendix A. U-values of the standard constructions are compared with Boverkets building regulations 22 according to Boverket (2015) to fulfil their recommendations, and if not the insulation thickness is adjusted.

As mentioned above, the floor is a light-weight construction with wooden beams, placed with a centre-to-centre distance of 600 mm with mineral wool insulation between, see Figure 4.2. To archive a better heat distribution of the light-weight floor, as discussed in Section 3.1, heat conductive plates are inserted next to the water pipes.

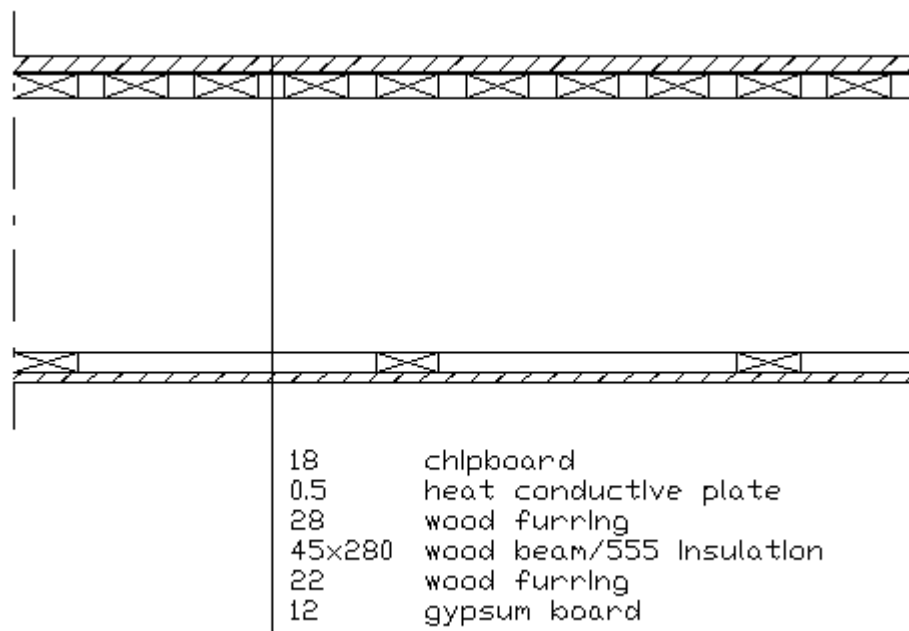| 18 | chipboard |
0.5	heat conductive plate
28	wood furring
45x280	wood beam/555 insulation
22	wood furring
12	gypsum board

Figure 4.2 Geometry and material of floor construction in Standard room

The recommended U-value according to Boverket (2015) for a floor construction placed on the ground is 0.15 W/m^2. To fulfil this recommendation the insulation needs a height of 280 mm, which result in a total floor height of 360 mm. According to Karlsson[4], the insulation thickness of the floor should be at least 250 mm to obtain a good insulation efficiency of the floor. Due to the low difference in insulation thickness, the thickness needed to fulfil Boverket is kept.

The heat demand of the standard room is 232 W which is 25 W/m^2, while having an indoor temperature of 22 °C and an outdoor temperature of -16 °C, see Appendix B. The floor heating system in the Standard room is calculated according to the semi-analytical calculation method presented in Section 3.2. This results in an upward and downward heat flux of

---

[4] Henrik Karlsson (Researcher, SP Technical Research Institute of Sweden) lecture in Building Physics Advanced April 29th 2015

$\gamma_{up} = 0.661 \text{ W/m}^2\text{K}$ and $\gamma_{down} = 0.026 \text{ W/m}^2\text{K}$, and an insulation efficiency of $\eta = 0.962$, see Appendix B. The Standard room's floor construction is a well-insulated floor according to the criterion of insulation efficiency in Section 3.2.

4.3 Reference model

The reference model in COMSOL Multiphysics 5.2 is simulated by the Heat Transfer Module and Pipe Flow Module. With Heat Transfer Module and Pipe Flow Module, the influence of heat transfer in solid materials is studied as well as heat transfer in pipes with fluid flow.

The reference model is a steady-state 3D model and represents the floor construction from the standard room. More about its geometry, materials and boundary conditions in COMSOL Multiphysics is presented in the following sections.

4.3.1 Geometry

The geometry and dimensions of the reference model is the same as for the standard solution and consist of domains by rectangles and polygons representing solid layers, see Figure 4.3. The pipe is model as a polygon, and simulated as a pipe with flowing fluid by Pipe Flow module.

The heat conductive plate is significantly thinner than the rest of the domains. If the mesh is larger than the domain, numerical error might occur. Instead, the boundary condition Thin Layer is used to model the heat conductive plate, described in Section 4.3.3.1. Furthermore the heat conductive plate is assumed to be homogenous; it is to say have no airgaps between the plates. This assumption applies for other layers such as furring. The impact of this assumption is discussed by a comparison with a non-homogenous version of the reference model in Section 4.3.5.3.
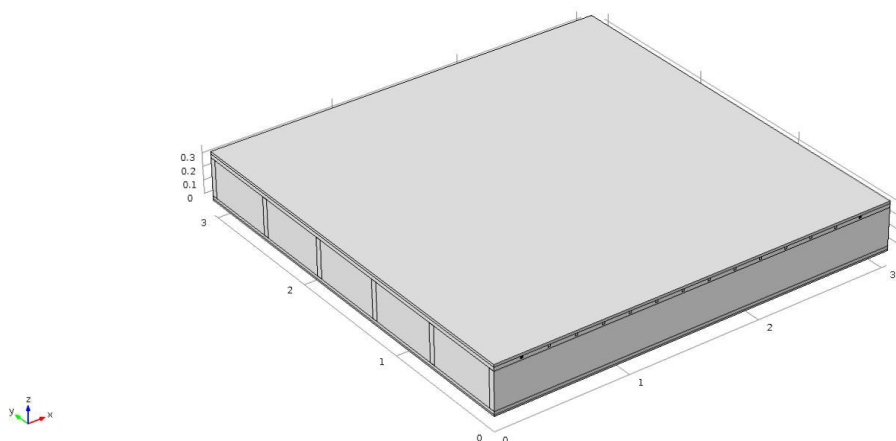

Figure 4.3 Homogenous model with geometry from Standard room in COMSOL Multiphysics 5.2

4.3.2 Materials

The assigned materials and their properties are assumed to be constant values, hence not to depend on temperature variations, to decrease simulation time, see Table 4.1. All geometries, which are modelled as a domain, are assigned a material, see Figure 4.4. As mentioned above, a part of the heat conductive plate is modelled by the boundary condition Thin Layer and the pipe is modelled as a polygon thus not visible in Figure 4.4 below.

Table 4.1 Materials and its properties inserted into reference model in COMSOL Multiphysics

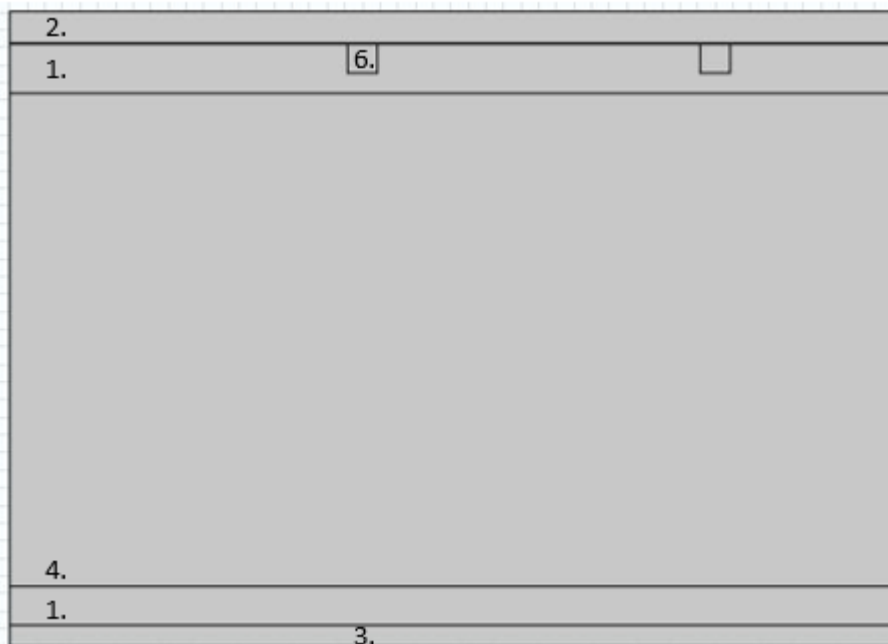| No.	Material	Thermal conductivity, λ [W/mK]	Density, ρ [kg/m^3]	Specific heat capacity, c_p [J/kgK]
1	Wood	0.14	500	1500
2	Chipboard	0.13	500	1500
3	Gypsum board	0.22	900	800
4	Insulation Mineral wool	0.04	100	800
5	Water	0.60	1000	4200
6	Heat conductive plate Aluminium	200	2700	900

Figure 4.4 Placement of material in Reference model in COMSOL Multiphysics 5.2

For water, which is the medium in the pipe, the ratio of specific heat is needed to run the Pipe Flow module. The ratio of specific heat is the ratio between specific heat at constant pressure and specific heat at constant volume, according to equation (4.1) (Engineering Toolbox, 2016).

$$\gamma = \frac{c_p}{c_v} \quad [-] \tag{4.1}$$

Further, dynamic viscosity of the water needs to be inserted into the Pipe Flow module. The parameters are as well as other properties varying with the temperature, but to decrease the simulation time, the values are considered to be constant, see Table 4.2.

Table 4.2 Properties of water required by Pipe Flow module inserted into reference model in COMSOL Multiphysics

Material	Ratio of specific heats, γ [-]	Dynamic viscosity, M [Pa*s]
Water	1,33	0,653

4.3.3   Boundary conditions

Boundary conditions are assigned to the model by the two physics; Heat Transfer in Solids or Heat Transfer in Pipes. The boundary conditions can be internal condition, such as Heat Transfer in Solids, to obtain conductive heat transfer in and between the geometries. And it can also be external conditions to prescribe the heat exchange to the surroundings.

More information about these physics and the prescribed boundary conditions is presented in the following sections.

4.3.3.1   Heat transfer in solids

All solid geometries in the model are assigned the physic Heat Transfer in Solids to create heat transfer by conduction in and between the different parts, according to equation (4.2) and equation (4.3). It is assumed that heat transfer only occurs from the top and bottom of the floor while the other sides are adiabatic, thus assigned to the boundary condition Thermal Insulation according to equation (4.4).

$$\rho c_p \boldsymbol{u} \nabla T + \nabla(\boldsymbol{q}) = Q \tag{4.2}$$

$$\boldsymbol{q} = -k \nabla T \tag{4.3}$$

$$q_0 = 0 \tag{4.4}$$

At the upper and lower part of the floor construction, the boundary condition Convective Heat Flux is assigned according to equation (4.5). The external temperature, T_e, in this case is the indoor temperature and T is the floor surface temperature. The heat transfer coefficient, h, represents both the convective heat transfer coefficient and radiative heat transfer coefficient. From previous Section 3.1, the convective and radiative heat transfer coefficient is decided by Figure 3.1 and Figure 3.2.

$$q_0 = h(T_e - T) \tag{4.5}$$

In the diagrams, the convective heat transfer coefficient varies with the temperature difference between floor surface and indoor air. Hence this needs to be regulated while getting result of the temperature of the floor surface. At the same time, the radiant heat transfer coefficient is constant.

Very thin domains compared to the overall geometry, such as the heat conductive plate with a thickness of 5 mm, is modelled by the boundary condition Thin Layer. Instead of creating a domain and applying a very small mesh size, the domain is modeled as a layer, which decreases both simulation time and possible numerical errors. In the boundary condition, the layer type conductive is chosen where the layer thickness, d_s, and layer thermal conductivity, k_s, are prescribed according to equation (4.6) and equation (4.7).

$$-\boldsymbol{n} \cdot \boldsymbol{q} = -\boldsymbol{\nabla}_t \boldsymbol{q}_s \tag{4.6}$$

$$\boldsymbol{q}_s = -d_s k_s \boldsymbol{\nabla}_t T \tag{4.7}$$

4.3.3.2 Heat transfer in pipes

The polygon representing the pipe is assigned with the physic Heat Transfer in Pipes, to create heat transfer into the pipe and to its surroundings according to equation (4.8).

$$\rho A c_p \boldsymbol{u} \cdot \nabla_t T = \nabla_t \cdot A k \nabla_t T + f_D \frac{\rho A}{2 d_h} |\boldsymbol{u}|^3 + Q_{wall} \tag{4.8}$$

The left term is heat transfer due to fluid flow and the first term on the right side due to conduction. Further, the second term on the right side is due to fiction heat by viscous heat (COMSOL, 2015). Viscous heat is heat produced due to shear forces acting on nearby layers (Morini, 2013). The parameter Q_{wall} describes heat exchange through pipe wall, presented below.

The input tangential velocity, u, in equation (4.8) is prescribed manually in the boundary condition Pipe Properties. This boundary condition also defines other properties and equations of the pipe, such as its shape, flow resistance and surface roughness.

The pipe's outlet is assigned to the boundary condition Heat Outflow, which takes convective heat transfer into account (COMSOL, 2015). Further, the inlet of the pipe is a fixed temperature and assigned with the boundary condition Temperature, according to equation (4.9).

$$T = T_{in} \tag{4,9}$$

When assigning an inlet water temperature, the temperature in the point representing the pipe's inlet is decreased by the Pipe Flow module. This might be due to a temperature distribution within the cross section. Therefore the

assigned inlet water temperature needs to have a higher value to get the wanted mean temperature at the pipe's inlet, see Figure 4.5.
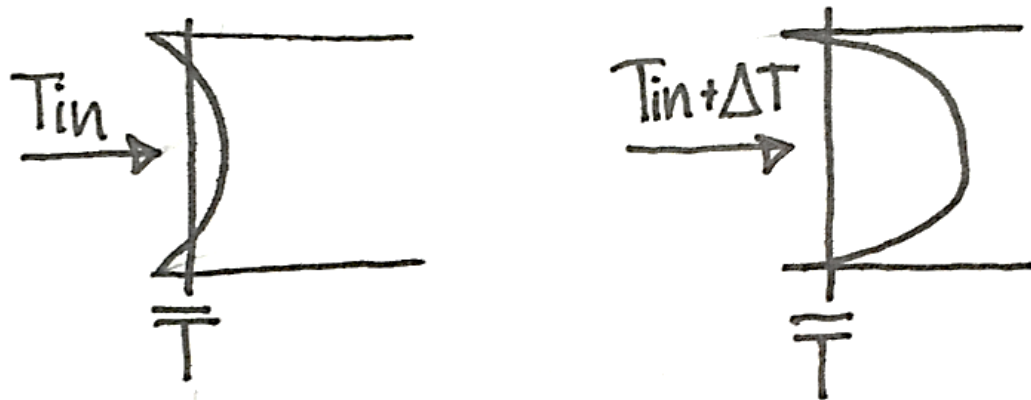

Figure 4.5 Temperature distribution within the cross section of the pipe inlet

Heat transfer through the pipe wall is assigned by the boundary condition Wall Heat Transfer according to equation (4.10). Where T_{ext} is assigned to the temperature surrounding the pipe wall, hence the temperature given by the physics Heat Transfer in Solids. The parameter $(hZ)_{eff}$ is the overall heat transmittance and depends on the cross section. Due to the circular cross section this is calculated according to equation (4.11).

$$Q_{wall} = (hZ)_{eff}(T_{ext} - T) \tag{4.10}$$

$$(hZ)_{eff} = \cfrac{2\pi}{\cfrac{1}{r_0 h_{int}} + \cfrac{1}{Z_N h_{ext}} + \Sigma\left(\cfrac{ln\left(\frac{r_n}{r_{n-1}}\right)}{k_{wall,n}}\right)} \tag{4.11}$$

4.3.4   Investigated models

Three different models are investigated to simulate the floor heating system. The models aims to use as less prescribed parameters as possible, to decrease the influence on it. The investigated models are; a model of the floor construction, a model of the floor construction with air box placed above and a model of the floor construction as well as external wall.

The first model represents the floor construction with embedded floor heating system, see Figure 4.6. In this model the heat transfer coefficient, calculating the heat flow rate from the upper and lower surface of the floor construction is prescribed, according to Section 3.1.
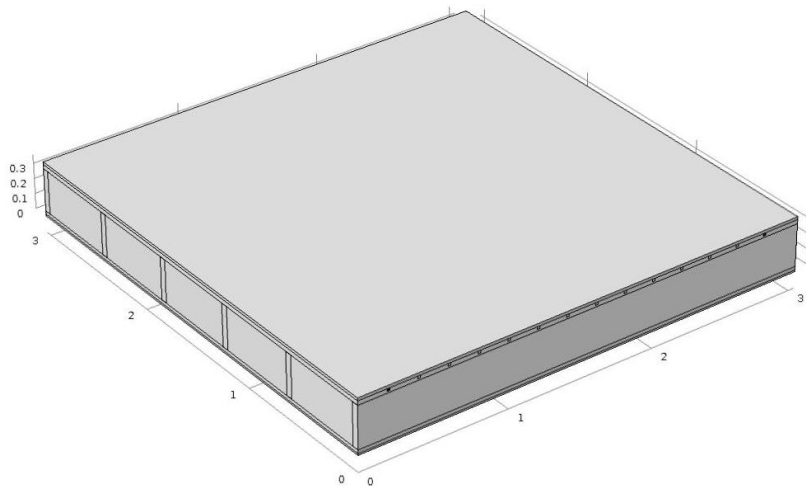
Figure 4.6 COMSOL Multiphysics model representing floor construction with embedded floor heating system

The second model consists of the floor construction with embedded floor heating system and an added air box on the upper floor surface, see Figure 4.X. With this model, the prescribed upper heat transfer coefficient is avoid due to the air box. It is most important to avoid the upper heat transfer coefficient, because the biggest amount of heat is released through the upper floor surface. On the air box the sides are considered be adiabatic except from the side representing the external wall which has an assigned heat flux representing the heat transfer through the wall.
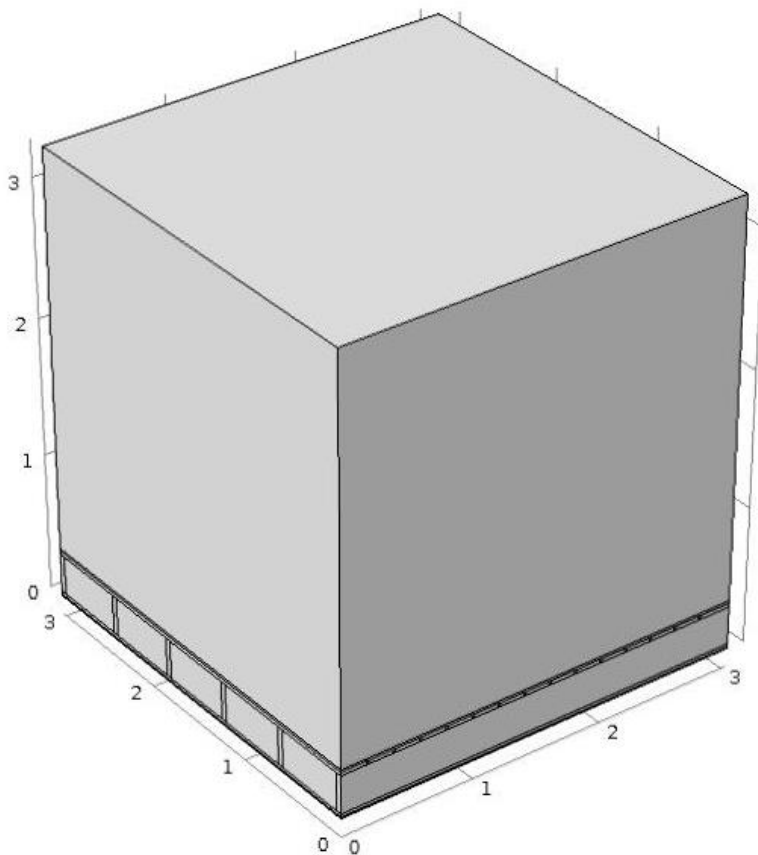

Figure 4.7 COMSOL Multiphysics model representing floor construction with embedded floor heating system and added air box

The third model consists of the floor construction with added air box and the external wall of the standard room, see Figure 4.X. By adding the external wall, the prescribed heat flow rate through the wall is avoided. Instead the heat transfer coefficient represents the combined surface resistances in Section 2.3.
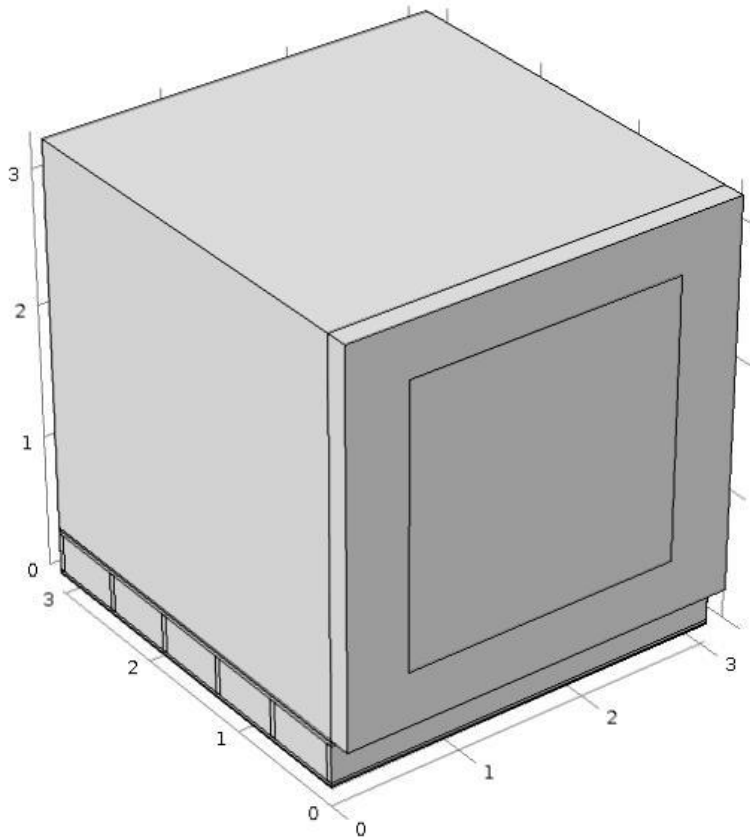

Figure 4.8 COMSOL Multiphysics model representing floor construction with embedded floor heating system and added air box and external wall

When simulating the models with an air box without CFD simulations, the air box acts like an insulated layer due to the low thermal conductivity of air. Therefore, the floor heating system was not represented correctly by using these models. Due to lack of time and complexity of the model, CFD simulations was not investigated further instead the investigation continued with using only the floor construction with embedded floor heating system.

4.3.5 Modelling result of Reference model

The inlet water temperature and water velocity parameters is inserted into COMSOL Multiphysics to study the reference model, as mentioned above. When simulating, results such as outlet water temperature, floor surface temperature and heat flow rate from the floor construction, is obtained. To fulfil the heat demand of the standard room, an iterative process evaluates required inlet water temperature and water velocity. The iterative process consists of two steps; first calculate γ_{up} and γ_{down} and then use the upward and downward heat fluxes to evaluate the inlet water temperature and water velocity.

The parameters γ_{up} and γ_{down} are calculated iteratively according to equation (3.4) and equation (3.5). The iterative process starts with simulating the reference model with inlet water temperature of $T_{fluid} = 1^oC$, indoor temperature of $T_{indoor} = 0^oC$ and estimated water velocity to obtain heat flow rate and outlet water temperature. Further, the upward respectively downward heat flow rate is divided with the pipe length to obtain upward and downward heat flux by equation (3.4) and equation (3.5). The upward and downward heat flow rate is divided with the pipe length because the 2D model in the semi-analytical calculation method represents the pipe length. With simulated results, the estimated water velocity is calculated according to equation (4.12). Where the mass flow rate is expressed by equation (3.3), with simulated results of heat flow rate and temperature decrease along the pipe.

$$u = \frac{V_f}{A_{pipe}} \ [m/s] \qquad (4.12)$$

This process of calculating upward and downward heat flux, continues until an error less than three decimals is obtained. This iterative process results in $\gamma_{up} = 0.515$ W/mK and $\gamma_{down} = 0.021$ W/mK. Furthermore, the insulation efficiency of the reference model is calculated to $n = 0.960$.

The second step consist of calculating the inlet water temperature and water velocity to achieve the required heat demand of 232 W. The process is similar to the one described above, but instead the heat fluxes and insulation efficiency is known. Initially, the inlet water temperature and water velocity is estimated to obtain simulated results of heat flow rate and outlet water temperature. Further, the water velocity is calculated according to equation (3.3) and equation (4.12), before inserted into the in-depth numerical model for another simulation. The process continues until the heat demand is accomplished, which results in a required inlet water temperature of $T_{fluid} = 34 \ ^oC$ and water velocity of $u = 0.039$ m/s.

4.4   Verification of Reference model

To ensure the reference model is reliable, a verification of the results is done. The verification consists of first comparing the Reference model with the calculation method, described earlier in Section 3.2, followed by a verification of the mesh influence, to investigate possible numerical errors.

More information about the verifications and its results is presented and analysed in the following sections.

4.4.1   Verification to calculation method

The reference model is verified by comparing results obtain by simulations and calculation method of the standard room. The verification aim to discover possible differences and what consequences that follows.

Table 4.3 Comparison of result given by calculation method of standard room and result given by simulation of reference model

Parameter	Calculation method	Reference model	Difference
γ_{up} [W/mK]	0.661	0.515	0.146
γ_{down} [W/mK]	0.026	0.021	0.005
η [−]	0.962	0.960	0.002

The differences between the reference model and calculations of the standard room are seen in Table 4.3. The upward and downward heat flux differs by 22% respectively 19% while the differences of insulation efficiency is a decrease of 2%. With a minor difference in insulation efficiency, the reference model distribute similar proportion of heat upward and downward as the calculation method. Moreover the reference model requires more heat to obtain the same heat flow rate compared to calculated result, due to significant difference in heat fluxes.

The explanation of the difference above is connected to the discussion about the temperature distribution by the Pipe Flow module in Section 4.3.3.2, where the temperature distribution within the pipe cross section is differing. The decrease of heat fluxes in the reference model is due to a lower mean water temperature in the pipe compared with the assigned temperature in the hand calculations.

If the theory described above is correct, similar heat conductance of the reference model can be achieved by increasing the temperature of the water close to the pipe wall. An alternative is to increase the water velocity, hence create a quicker exchange of the water close to the wall. If the water velocity of the reference model is increasing to 0.25 m/s similar heat conductance is achieved, see Table 4.4. The differences in heat conductance between hand calculation and reference model is instead 2 %, while the insulation efficiency still has a difference of 0.2 %. The insulation efficiency is not affected is because it is connected to the floor construction.

Table 4.4 Result compared to hand calculations while increasing water velocity of reference model

Parameter	Calculation method	Reference model with $u = 0.25$ m/s	Difference
γ_{uo} [W/mK]	0.661	0.648	0.013
γ_{down} [W/mK]	0.026	0.027	-0.001
η [−]	0.962	0.960	0.002

4.4.2   Verification of mesh size

By verifying the mesh size, possible numerical error of the model is identified. The model contains numerical error if the result differs depending on the mesh size. To only obtain possible dissimilarities influenced by the mesh, an identical model is simulated.

The mesh size is solved by the automatic mesh building tool in COMSOL Multiphysics, called physics-controlled mesh, and the element sizes goes from Extremely Coarse to Extremely Fine. The mesh size Coarse creates to big elements to fit into the domains hence creates numerical errors. The Extremely Fine mesh size requires more computer capacity than what is available in the study. Therefore, only the sizes Normal to Extra Fine are investigated, see Table 4.5.

Table 4.5 Results from reference model with difference mesh sizes

Mesh Size	Number of elements	Calculation time	Q_{up} [W]	Q_{down} [W]	$T_{floor,surface}$ [^{o}C]
Normal	194 469	1 min 25s	231.15	9.60	25.02
Fine	508 520	3 min 26s	231.06	9.59	25.02
Finer	1 247 237	9 min 16s	230.93	9.58	25.02
Extra fine	2 007 191	17 min 42s	230.93	9.58	25.02

According to Table 4.5 the differences in results between the investigated mesh sizes are small, which indicates that the model does not contain any numerical errors. But differences in calculation time are greater between the mesh sizes. Due to similar results, the mesh size that requires less calculation time, in this case Normal mesh size, is chosen without the risk of getting numerical errors.

4.5 Comparison with non-homogenous model

An assumption to simulate layers as homogenous without airgaps was mentioned in Section 4.3.1. Instead of the homogenous layers, the parts with a centre-to-centre distance, such as furring and heat conductive plates, is modelled with air between, see Figure 4.6.
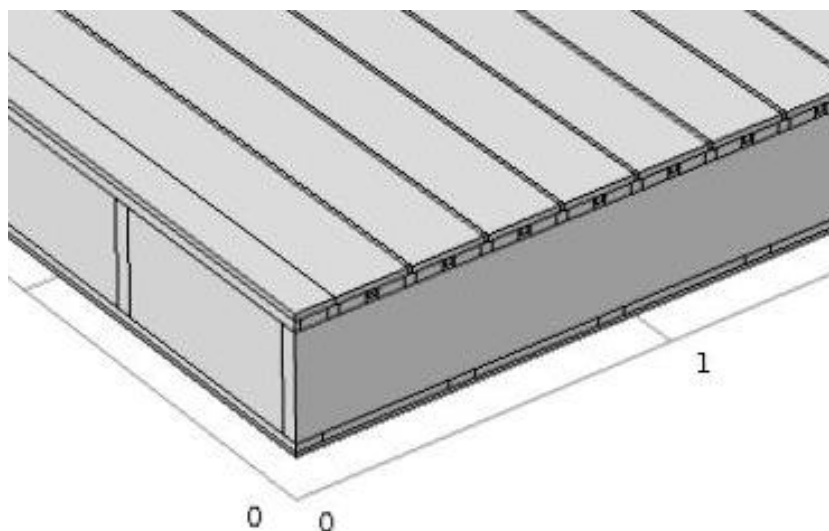

Figure 4.9 Non-homogenous model of Standard room in COMSOL Multiphysics 5.2

The assumption aims to create a model with faster calculation time, especially when an advancer model might be required. Another reason is to decrease the amount of domains containing air as material, due to the low thermal conductivity of air, $\lambda = 0.025$ W/m^{2}K. Therefore, domains with air as material are receiving incorrect properties similar to a well-insulated domain. With regard to this, two non-homogenous models are simulated; one with air as an ordinary domain and one with air as an isothermal domain. To only get the difference caused by the domain structure, the model have the same input data, see Table 4.6.

Table 4.6 Comparison of homogenous model, non-homogenous model and non-homogenous model with isothermal domain

Model	Calculation time	Q_{up} [W]	Q_{down} [W]	η [−]	$T_{floor,surf}$ [^{o}C]	T_{outlet} [^{o}C]
Homogenous	1 min 27s	231.2	9.6	0.960	25.0	26.6
Non-homogenous	9 min 23s	217.6	8.2	0.964	26.5	26.9
Non-homogenous Isothermal	9 min 10s	217.9	5.3	0.976	26.5	27.0

In Table 4.6, an obvious difference between the homogenous model and the two non-homogenous models is received. Both upward and downward heat transfer is decreased, but the floor surface temperature is increased. This indicates that the non-homogenous models require more supplied heat to obtain wanted heat demand. Therefore the non-homogenous models have a lower thermal conductivity than the homogenous model, hence bigger difference to the hand calculations of the standard room. With regard to the heat conductance difference, a better option is to continue with the assumption of homogenous layers and be aware of the influence of the Pipe Flow module.

5 Numerical model of floor heating system in HSB Living Lab

5.1 HSB Living Lab

A living lab is an experimental environment used as a tool to perform real life research (Balaÿ, 2014). According to Balaÿ (2014), living lab is involving its users, because the users live in the research environment, and thereby innovations are tested in their working situation. Assign to the construction sector, future building technologies can be investigated and improved before released to the market.

HSB Living Lab is a project consisting of a transportable modular building, including both residential and commercial parts, which involves short and long-term research projects. From construction start in February 2016, the building is placed at Chalmers University of Technology in Gothenburg. The aim of the project is to obtain more sustainable awareness in the everyday life (HSB Living Lab, 2016). During ten years, which the project consists of, subjects such as architecture and movability, materials and technology and minimization of resources is researched together with 9 collaborators (HSB Living Lab, 2016).

The building consists of four stories which include tree residential (private) floors and one public bottom floor. The residential floors consist of 23 apartments, where each group of six apartments is sharing kitchen, balcony and a bathroom including shower (HSB Living Lab, 2016). The apartments have different sizes, where a one bedroom apartment is a cube of 47 m^3 with the size 3.6*3.6*3.6 m (HSB Living Lab, 2016). The apartment unit that will be investigated is on floor two facing south-west orientation, see marked apartment in Figure 5.1.
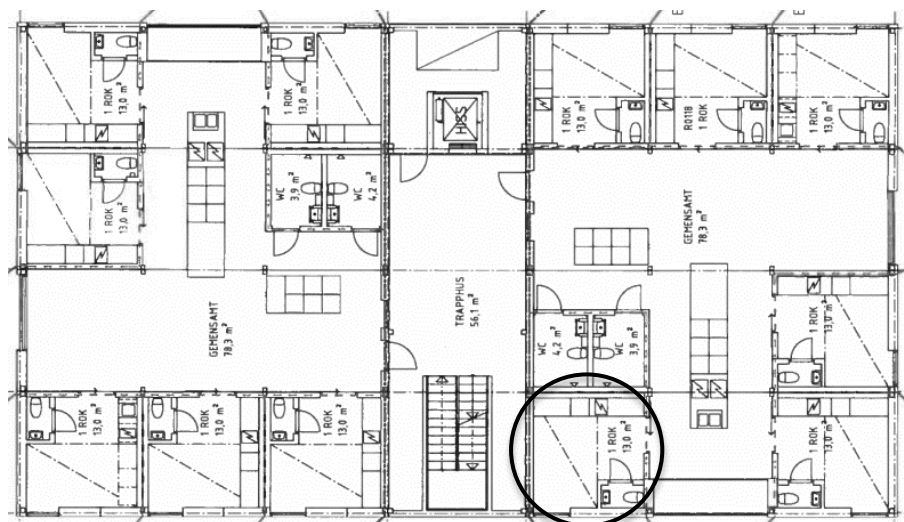

Figure 5.1 Floor plan of floor two and four in HSB Living Lab

The heating system on floor two and four consists of a water based floor heating system. Each apartment has an own circuit, that heats 7 m^2 of the floor area, with a center-to-center distance of 200 mm, see Figure 5.2.The indoor temperature is 20 ^{o}C with an inlet water temperature of 28 ^{o}C and a water velocity is depending

on each circuits heat demand. The water velocity in the investigated apartment unit is 0.47 m/s.
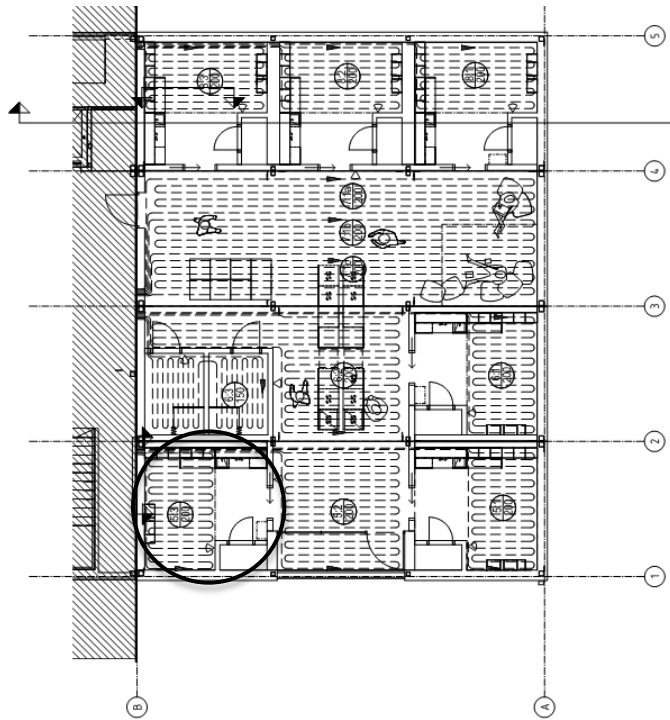

Figure 5.2 Floor heating system in one side of floor two and four in HSB Living Lab

The floor construction on floor two and four is a light-weight construction consisting of steel U-profiles, with rock wool insulation between, see Figure 5.3. The flooring above the floor heating system is wooden parquet, which is not seen in Figure 5.3.
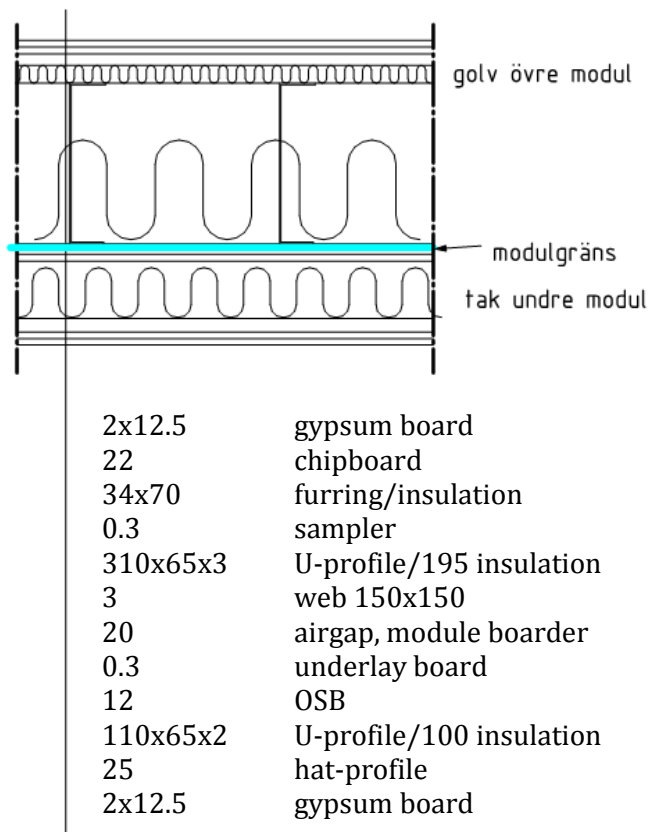
2x12.5	gypsum board
22	chipboard
34x70	furring/insulation
0.3	sampler
310x65x3	U-profile/195 insulation
3	web 150x150
20	airgap, module boarder
0.3	underlay board
12	OSB
110x65x2	U-profile/100 insulation
25	hat-profile
2x12.5	gypsum board

Figure 5.3Floor construction in HSB Living Lab

5.2 In-depth numerical model

The in-depth numerical model of the apartment unit in HSB Living Lab, called case study model, is modelled with the same physics and in the same approach as the reference model. The model is a 3D model of the floor construction from HSB Living Lab, but the case study model consists of both stationary and transient analysis. More about its geometry, material, boundary conditions and the different analyses is presented in the following sections.

5.2.1 Stationary and transient analyses

Compared to the reference model it is interesting to investigate how the floor performs when there are disturbances inside the apartment unit to study the self-regulation ability of the floor construction. The disturbance, which changes over time, can either be additional heat load caused by people, technical devices or by solar radiation.

When investigating the self-regulation ability, it is interesting to notice how quick the system adapts. Therefore, a simplified disturbance is interesting and not how well it applies to real-life situations. The simulated disturbance is of one and two persons heat load inside the apartment unit during certain time of five days, see Figure 5.4. The heat load represents a person in a sitting position that generates a heat load of 100 W/person. The first day consists of no heat load, thereafter one day with 100 W and then one day with 200 W. The time it takes to

adjust to the wanted heat load is assumed to be 3 hours. The slopes are needed to make the model adjust to heat load differences.
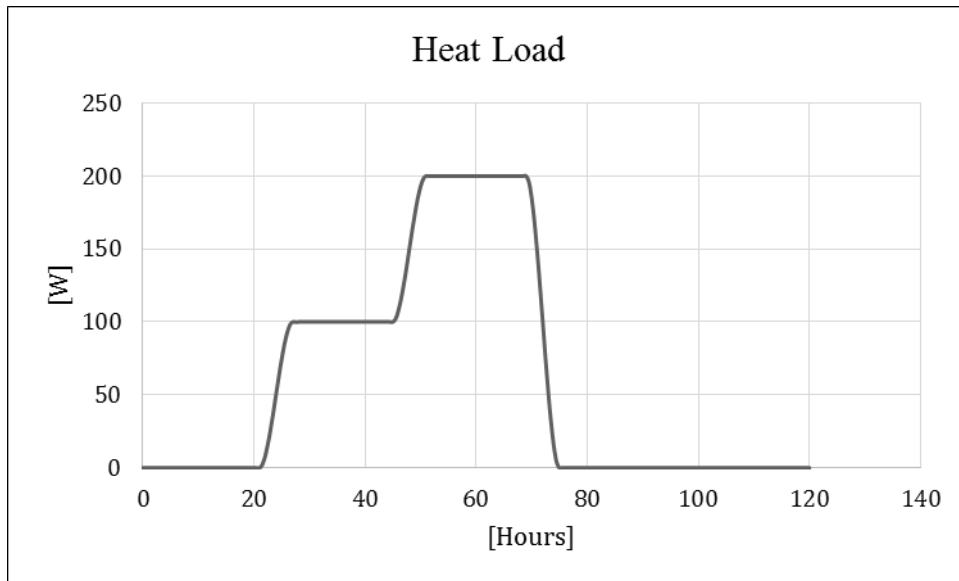

Figure 5.4 Disturbance caused by a heat load of one and two persons during 5 days

When applying a heat load in a volume, the temperature increases as well. Thereby an exponential indoor temperature is also simulated in the transient analysis, see Figure 5.5. The exponential indoor temperature is calculated according to equation (5.1).

$$T_{in}(t) = T_{out} + \left(T_{in,0} - T_{out}\right)e^{-t/t_c} \tag{5.1}$$

Where T$_{out}$, the temperature $T_{in}(T)$ is reaching, is assumed to be 25 °C and $T_{in,0}$ is 20 °C. The characteristic time, t_c, is calculated to be 65 h, to reach an temperature equal to the surface temperature when the last heat load ends.
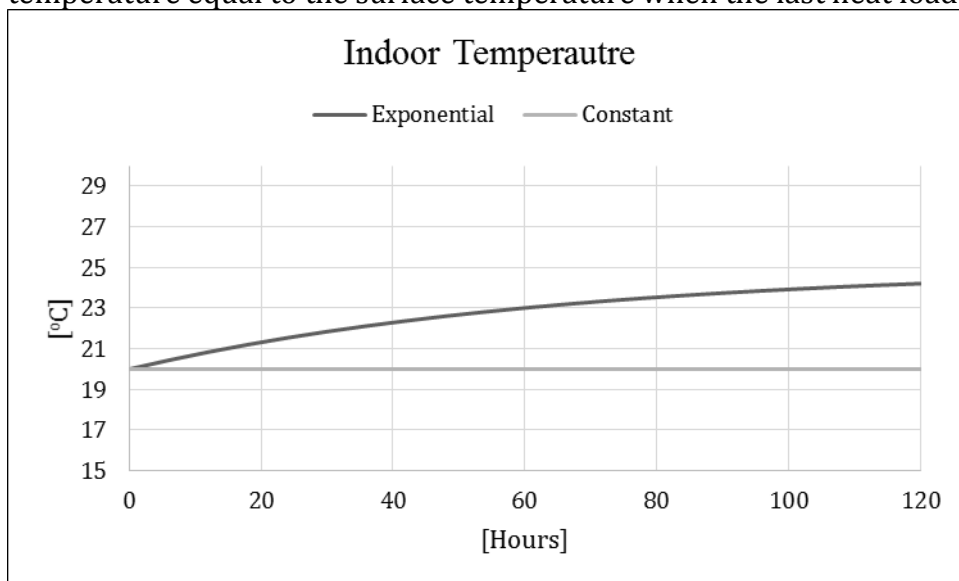
Figure 5.5 Exponential and constant indoor temperature

5.2.2   Geometry

The geometry of the in-depth numerical model is, as mentioned, the floor construction in the apartment units, see Figure 5.6. Similar to the reference model, the geometries are consisting of rectangles and polygons expressing solid layers. The steel hat profile in the bottom part of the construction is simplified to a homogenous layer. Furthermore, the thin U-profiles in steel is modelled by the application Thin Layer, described in Section 4.3.3.1. The insulation between the beams is simplified to be homogenous along the beam, instead of including an airgap. The thickness of the flooring is not presented in Figure 5.3, therefore assumed to a thickness of 15 mm.
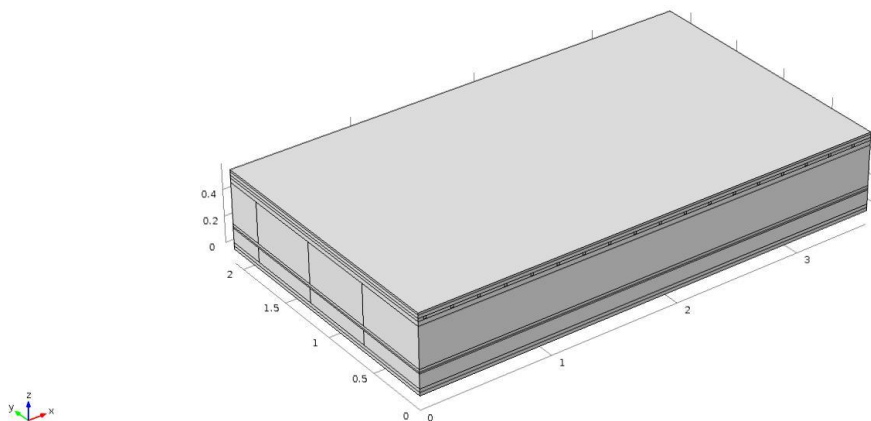
Figure 5.6 Stationary case study model of floor heating system in HSB Living Lab

The model is simplified to decrease simulation times while doing transient studies. The simplification aims to create a simpler model with less mesh elements. With smaller amount of mesh elements, the simulation time will be shorter. By modelling the under part of the floor construction as a homogenous layer, less mesh elements is obtained, see Figure 5.7. The thermal conductivity of the material is adjusted to obtain similar results as for the stationary case, see comparison in Appendix C.
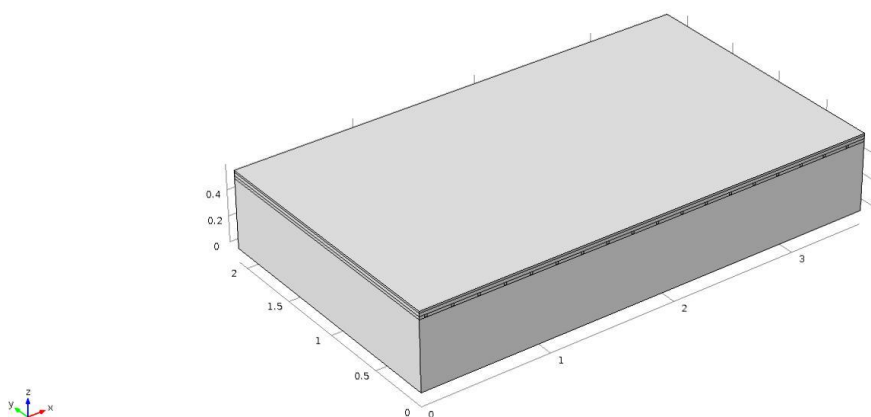

Figure 5.7 Simplified transient case study model of floor heating system in HSB Living Lab

5.2.3 Materials

As for the Reference model, the material properties are assumed to be constant values, see Table 5.1. The geometries modelled as domains are assigned properties by materials, see Figure 5.8.

Tabell 5.1 Material properties inserted into case study model

No.	Material	Thermal conductivity, λ [W/mK]	Density, ρ [kg/m³]	Specific heat capacity, c_p [J/kgK]
1	Wood	0.14	500	1500
2	Chipboard	0.13	500	1500
3	Gypsum board	0.22	900	800
4	Insulation Mineral wool	0.04	100	800
5	Water	0.60	1000	4200
6	Heat conductive plate Aluminium	200	2700	900
7	Steel, strainless	20	7800	500
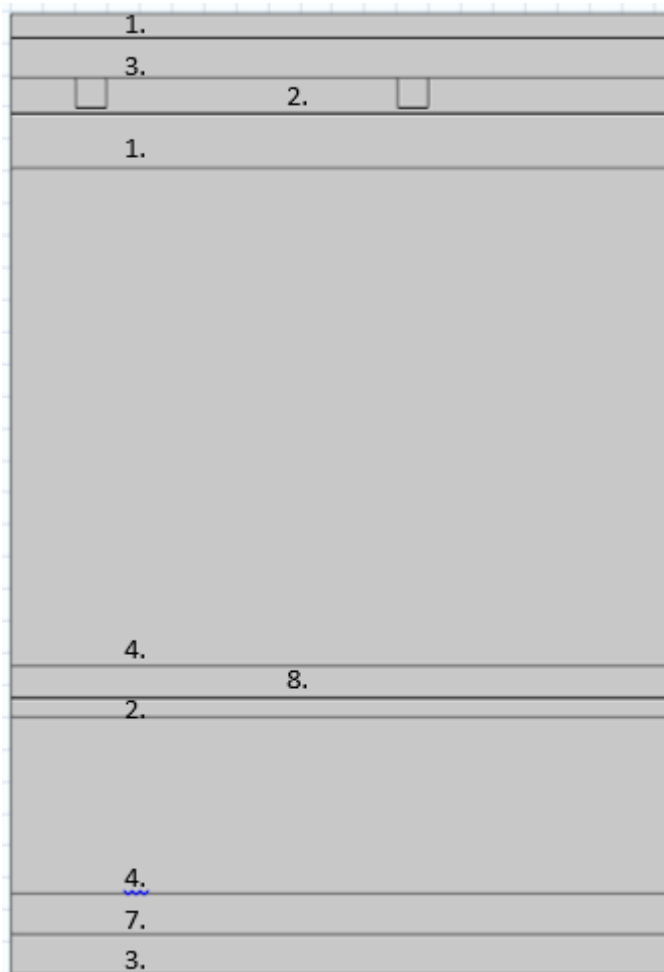
Figure 5.8 Placement of materials in case study model

The ratio of specific heat and the dynamic viscosity of the pipe medium, in this case water, are required in the Pipe Flow module. The properties are the same as for the reference model, see Table 4.2.

5.2.4   Boundary conditions

The boundary conditions of the case study model are almost similar to the reference model, such as Convective Heat Flux, Thin Layer and Wall Heat Transfer presented in Section 4.3.3. But when studying transient analyses, energy conservation is taken into account by the physics Heat Transfer in Solids and Heat Transfer in Pipes. Therefore equation (2.1) is added to equation (4.1) and (4.7). Furthermore, one boundary condition is added to the case study model to represent the transient disturbance.

The transient disturbance is assigned as the boundary condition General Inward Heat Flux, according to equation (5.2), and simulates a heat flux added on the floor surface. The heat flux represents the heat load mentioned earlier in Section 5.2.1, see Figure 5.4.

$$q_0 = q \qquad\qquad\qquad (5.2)$$

5.2.5   Modelling results of apartment unit

With the input data, mentioned in Section 5.2, inserted into the stationary model the upward heat is $Q_{up} = 113.3$ W, downward heat transfer is $Q_{down} = 4.3$ W and outlet water temperature is $T_{fluid,outlet} = 24.8$ °C. Hence a temperature drop of $\Delta T_{fluid} = 3.2$ °C along the pipe circuit. By an investigation of the floor surface temperature, it shows that the temperature in the stationary analysis never exceed the criterion of $T_{surf} > 27$ °C, see Figure 5.9.
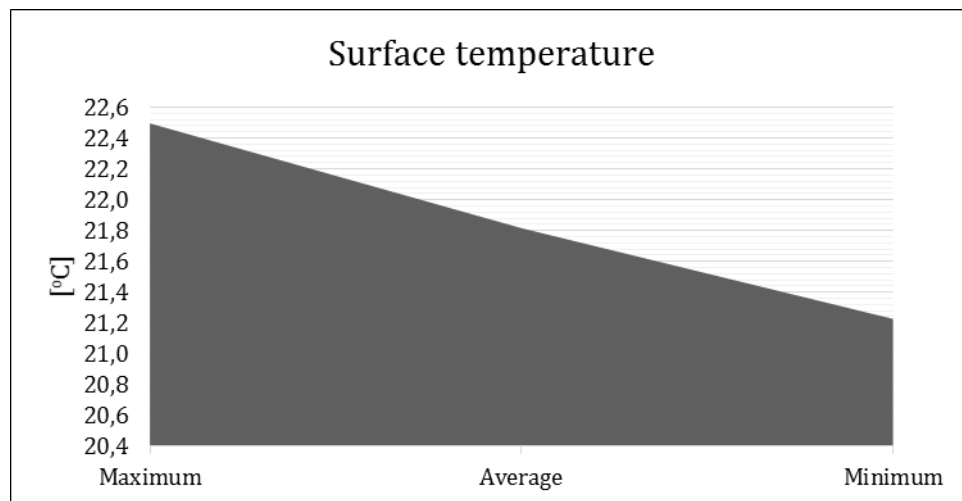

Figure 5.9 Floor surface temperature of case study model when simulated stationary

The ability of the case study model to adapt to disturbances inside the apartment unit is investigated by transient analyses of upward heat transfer, average floor surface temperature and outlet water temperature, see Figure 5.10, Figure 5.11

and Figure 5.12. The parameters adjust directly to disturbances indoors, which indicate on a self-regulation ability of the floor heating system
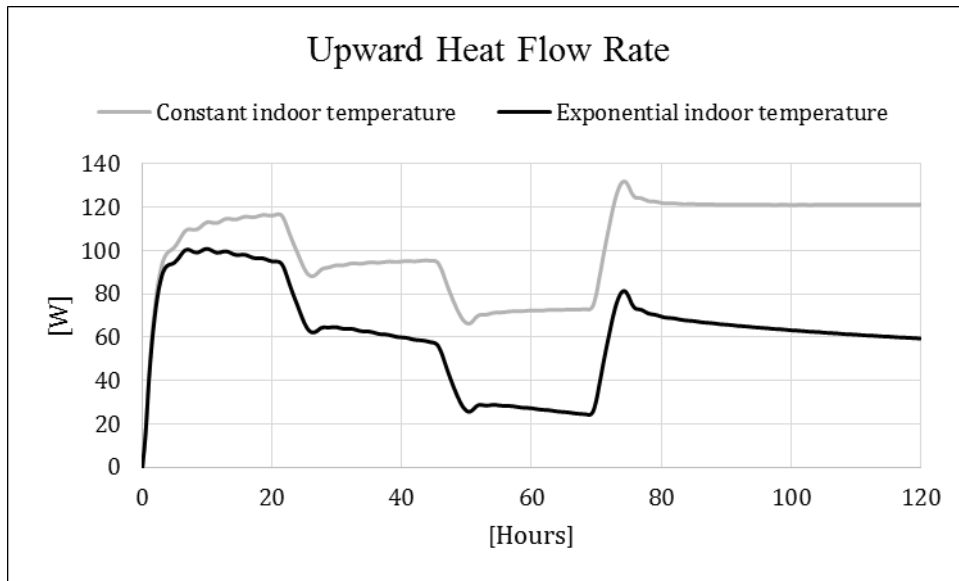

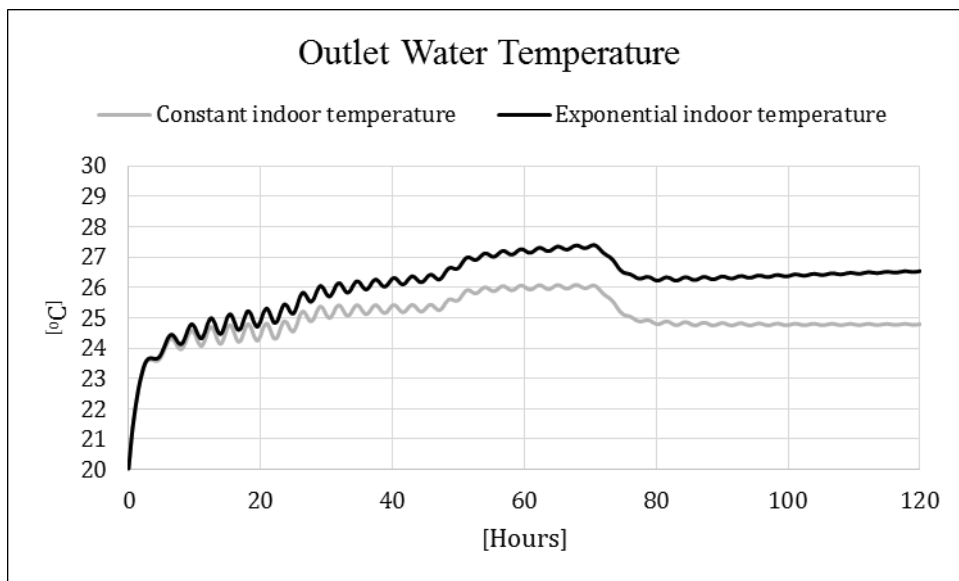*Figure 5.10 Heat transfer upward of transient analysis with positive disturbance*

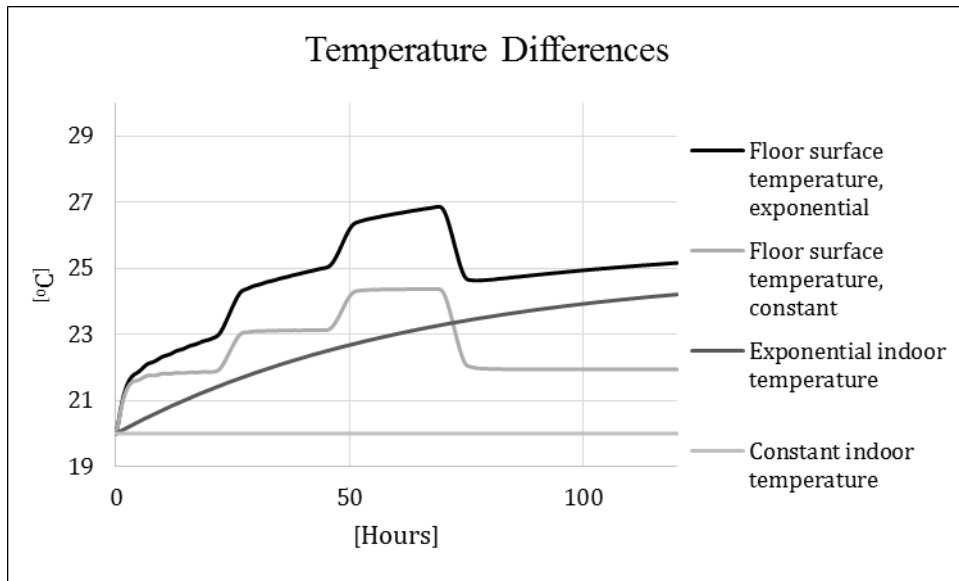*Figure 5.11 Outlet water temperature of transient analysis with positive disturbance*

Figure 5.12 Temperature differences between floor surface and indoor temperature of transient analysis with positive disturbance

Compared with the stationary upward heat transfer of 113.3 W, the supplied heat from the floor heating system is 95 W and 70 W at constant indoor temperature, when disturbance of one respectively two persons occur, see Figure 5.10. Combined with the heat load in the apartment unit, a total heat of 195 W and 270 W is obtained. Due to the increased floor surface temperature and constant indoor temperature, the heat supply from the floor heating system is increasing due to larger temperature difference, see Figure 5.12. The upward heat transfer is a combination of equation (4.3) and equation (5.2) hence calculated according to equation (5.3).

$$Q_{upward} = h(T_e - T) - Q_{load} \qquad (5.3)$$

When modelling with an exponential indoor temperature, the difference between the floor surface and exponential indoor temperature decreases, see Figure 5.12. This results in a decrease in upward heat flow rate as predicted, see Figure 5.10. Due to the decrease in upward heat flow rate, the outlet water temperature is increased as the self-regulation ability explains.

In future investigations, only constant indoor temperature is inserted into the model to decrease simulation time. Thereby, it should be taken into account that the simulated results has a higher upward heat flow rate and lower outlet water temperature and floor surface temperature than modelled with an exponential indoor temperature.

6 Investigation of potential improvements of floor heating system

When improving the floor heating system there are three improvements that are interesting to investigate, see Table 6.1. Each improvement contains an investigation on how the improvement can be simulated for further evaluations. By combining an improvement with another, benefits of different approaches might result in an even better performance improvement.

Table 6.1 Interesting improvements of floor heating system embedded into a light-weight construction

No.	Improvement	Investigation
1	Increase heat distribution from the floor construction	Change to a better heat distribution material
2	Increase thermal mass of the floor construction	Add screed as upper part of the floor construction
3	Increase thermal mass inside the apartment unit	Insert phase change material inside the room

Improvement one aims to increase the heat distribution from the floor construction by using a better heat distribution material, compared to previous heat conductive plate of aluminum. Further, the purpose of improvement two is to increase the thermal mass of the floor construction to obtain similar performance as a heavy-weight floor. The investigation consists of embedding the pipes into screed, hence changing the upper part of the floor construction. Improvement three, aims to obtain similar performance as a heavy-weight floor by increase the thermal mass in the apartment unit. By placing phase change material, heat can be stored and used when needed.

To compare and evaluate result of investigated improvements, the same input data needs to be used. Therefore, all inlet water temperature and water velocities are 28 ºC and 0.047 m/s. In the following sections, the improvements is presented, investigated and analyzed.

6.1 Improving heat distribution of the floor heating system

By improving the heat distribution of the floor heating system, less heat needs to be supplied to get the amount of heat wanted. Furthermore, the improvement creates a more uniform surface temperature and decreases cold surfaces.

To improve the heat distribution, the heat conductive plates are replaced with a material with better heat transfer properties. It is also an advantage if the replacing material is homogenous, and does not contain airgaps between the plates as the heat conductive plates, as in the right illustration in Figure 3.1. With a material without airgaps, the spread of heat will be better and not create cold surfaces where the airgap is, mentioned above. A product with these properties is a graphite grid, which is described and investigated in the sections below.

6.1.1 Graphite grid

Graphite grid is a thin woven grid, of the graphite fibres, placed above the water circuit to increase the heat distribution, see Figure 6.2.

Figure 6.1 Placement of graphite grid in floor heating system
http://www.varmemattor.com/wood.html

The material graphite is a material of carbon atoms, consisting of strongly bonded layers with weaker bonds between the layers (Rennie, 2016). Due to the chemical structure of graphite the material is anisotropic, which affects its ability to transfer heat in different directions (Pierson, 1993). According to Palmquist[5], the direction differences of the thermal conductivity are approximated according to Table 6.2.

Table 6.2 Material properties of graphite grid and aluminum

Material	Thermal conductivity, x/y-direction [W/mK]	Thermal conductivity, z-direction [W/mK]	Density, [kg/m³]
Graphite grid	450	5-6	1000
Aluminium	200	200	2700

With a considerably better ability to transfer heat along the yarns instead of trough it makes the grid a good theoretical improvement to distribute the heat. When comparing to previous heat conductive plate of aluminium the properties differs, see Table 6.2.

In the numerical model, the graphite grid is simulated as a Thin Layer, described earlier in Section 4.3.3.1. According to Palmquist[5], the interface between the top part of the pipe and the grid is enough to create an increased heat distribution. A study of the influence in heat transfer, if the interface is increased is also done. The increase consists of surrounding the pipe completely by the graphite grid.

---

[5] Lennarth Palmquist (CEO, XY Climate) interviewed by the writer May 12th 2016.

6.1.2   Stationary analysis with improved heat distribution

By stationary simulations, the heat transfer is decreased when inserting graphite grid above the circuit compared with case study, see Figure 6.2. When increasing the interface between pipe and grid, the upward heat transfer improves from previous simulation but only insignificantly compared with case study result. When comparing downward heat transfer, the graphite grid with increased interface has less downward heat transfer than case study even though the upward increased to some extent. Therefore, the insulation efficiency of this improvement is higher in association to the case study.
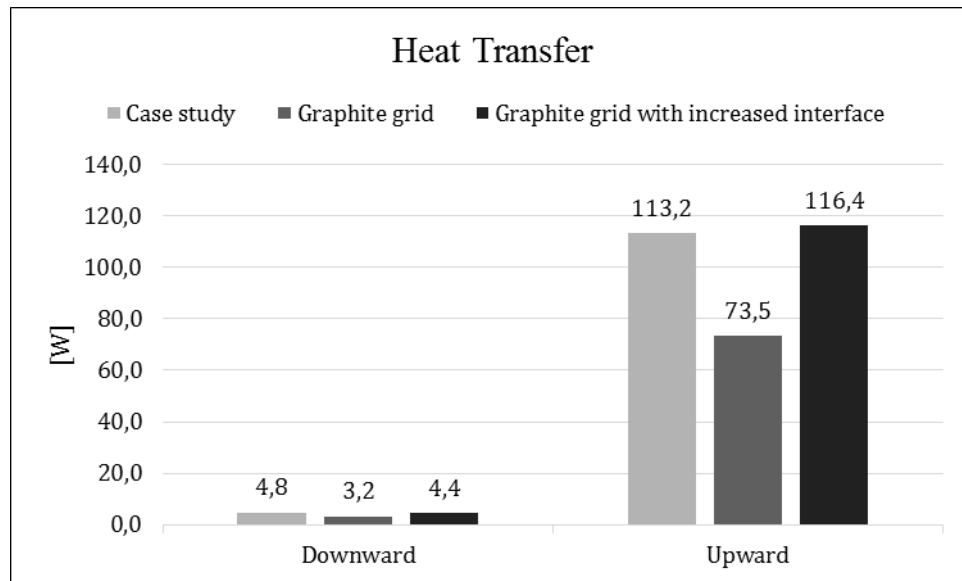
Figure 6.2 Upward and downward heat transfer with increased heat distribution

With the discussion above, the reason for the lower upward heat transfer of the graphite grid is a lower floor surface temperature in comparison with the case study, see Figure 6.3. With the lower heat transfer, the water temperature drop along the circuit is smaller; hence a higher outlet water temperature is obtained. By Figure 6.3, it is seen that the floor surface temperature of the graphite grid with increased interface is almost the same as the case study, hence similar upward heat transfer and outlet water temperature, see Figure 6.4.
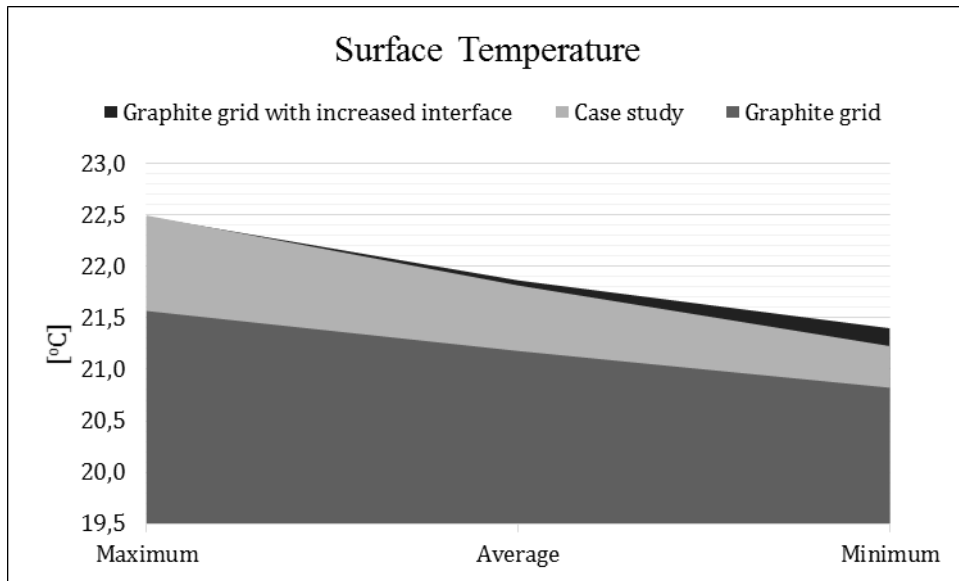
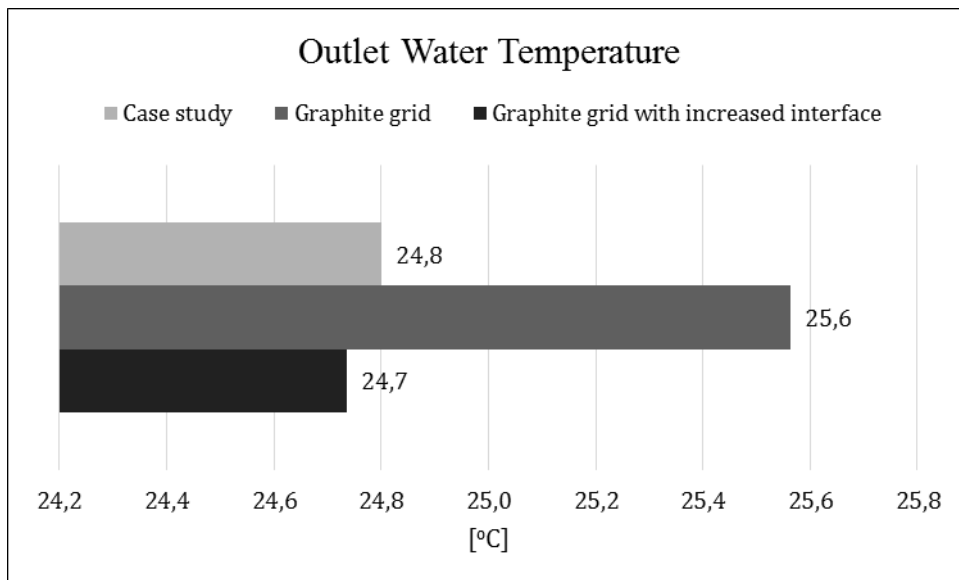*Figure 6.3 Surface temperature with increased heat distribution*

Figure 6.4 Outlet water temperature of increased heat distribution

By the evaluation above, the graphite grid without increased interface has poor results. Therefore, the transient analysis for this case is not performed. Instead, the solution with increased interface is analysed as presented below.

6.1.3 Transient analysis with improved heat distribution

According to the stationary analysis the upward heat transfer and the outlet water temperature are nearly unchanged compared with the case study, see Figure 6.5 and Figure 6.6. The difference is due to hourly variations where the case study model varies more and the graphite grid with increased interface is more stable. This might occur because the graphite grid is modelled anisotropic, while the previous heat distribution material had the same properties, hence changing the physical behaviour.
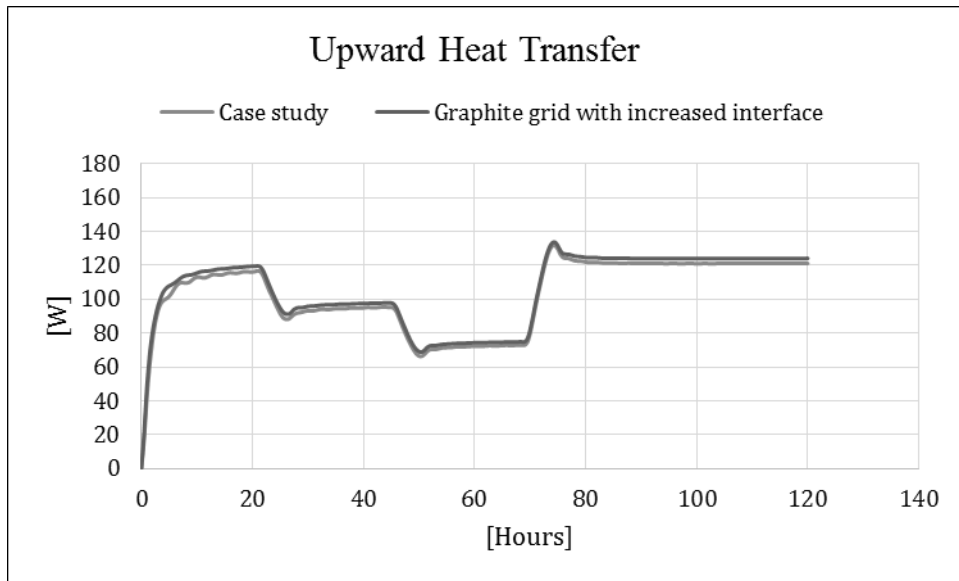
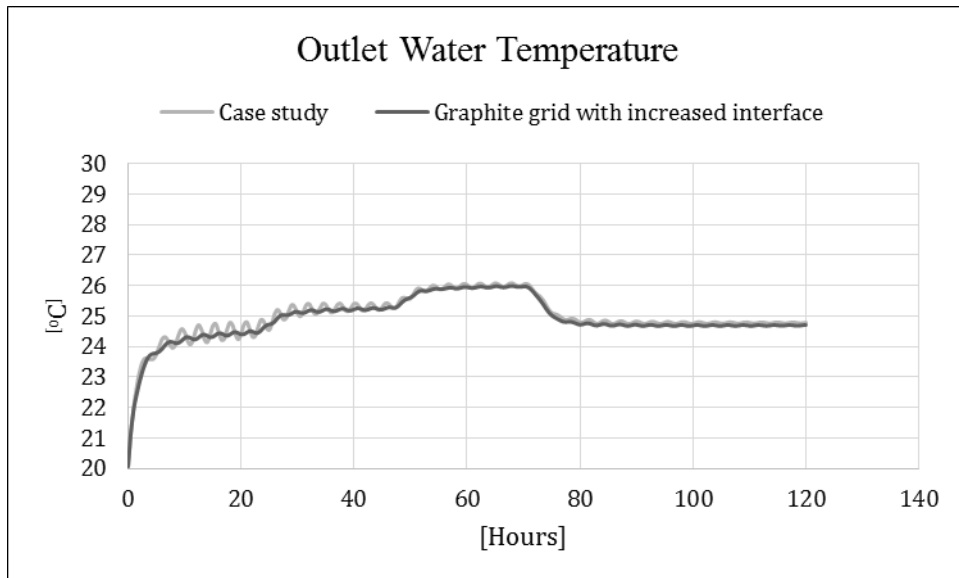*Figure 6.5 Upward heat transfer when simulating transient with increased heat distribution*

Figure 6.6 Outlet water temperature when simulating transient with increased heat distribution

6.2   Improving thermal mass of floor construction

The most energy efficient floor heating systems are when the pipes are embedded into heavy-weight floors, where the system takes advantage of the uniform heat distribution in and large amount of thermal mass. By improving the thermal mass of the floor construction, better abilities to store energy might occur (Karlsson, 2010).

A way of increasing the thermal mass of a light-weight floor construction with a floor heating system is to embed the floor heating system into screed instead of using chipboard and overlaying gypsum board. With this improvement, the top part of the floor construction is getting similar performance as a heavy-weight floor.

In the sections below, more information about screed is presented as well as investigated and analysed.

6.2.1 Screed

The pipes are embedded into the screed with a special rail, to prevent movement when casting, see Figure 6.7. The solution is typical in bathroom, because the screed can be casted to obtain a slope for water drainage. The pipes should at least be covered by 15 mm of screed, including floor coating (Uponor, 2016). In the numerical model, the screed is replacing the upper part of the floor construction, consisting of chipboard and two gypsum boards, with a total thickness of 47 mm. The flooring is the same as previous, consisting of 15 mm wooden flooring.

Figure 6.7 Floor construction with screed solution [Elektronisk bild]
https://www.uponor.se/vvs/system/golvvarme/forlaggning/rorhallarskena.aspx [Accessed 2016-05-23]

A well-known screed is Portland cement, which is used in the model. Due to large spread of thermal conductivities of cement, a cement with a higher thermal conductivity is also investigated, see Table 6.3.

Table 6.3 Material properties of screed

Material	Thermal conductivity, λ [W/mK]	Density, ρ [kg/m^3]	Specific heat capacity, c_p [J/kgK]
Portland cement	0.29	1522	1550
Cement with increased λ	1	1522	1550

6.2.2 Stationary analysis with improved thermal mass

When improving the thermal mass using Portland cement, the floor heating system is obtaining a declined heat transfer performance compared with the case study, see Figure 6.8. Further using Portland cement, less heat is released from the water pipe to the floor surface, resulting in the decrease in heat transfer, according to Figure 6.9 and Figure 6.10. When using a cement with increased λ, the heat transfer upward is increased and heat transfer downward decreased resulting in a better insulation efficiency of the floor construction, see

Figure 6.8. According to Figure 6.10, even more heat can be taken from the heated water due to lower outlet water temperate in the case study.
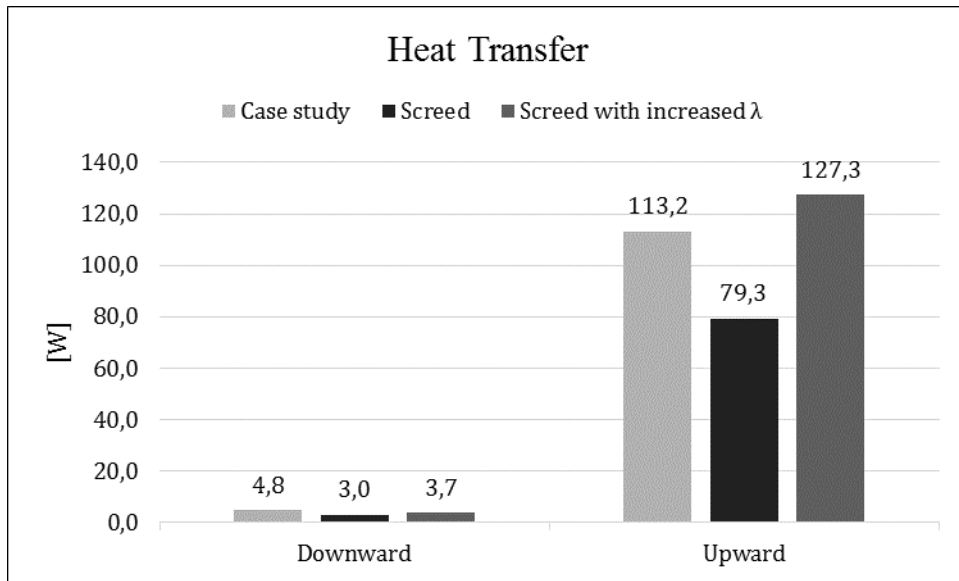

Figure 6.8 Upward and downward heat transfer of increased thermal mass in floor construction
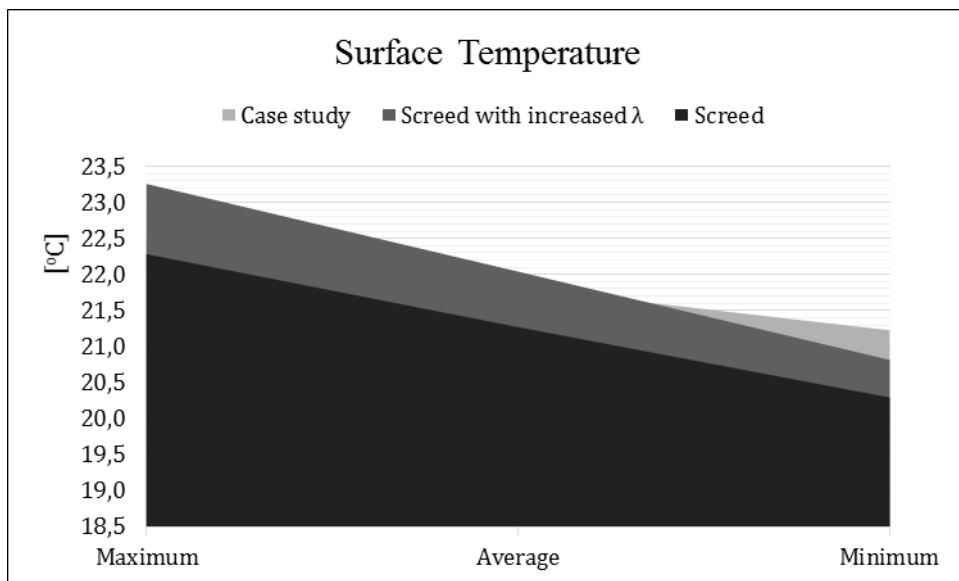

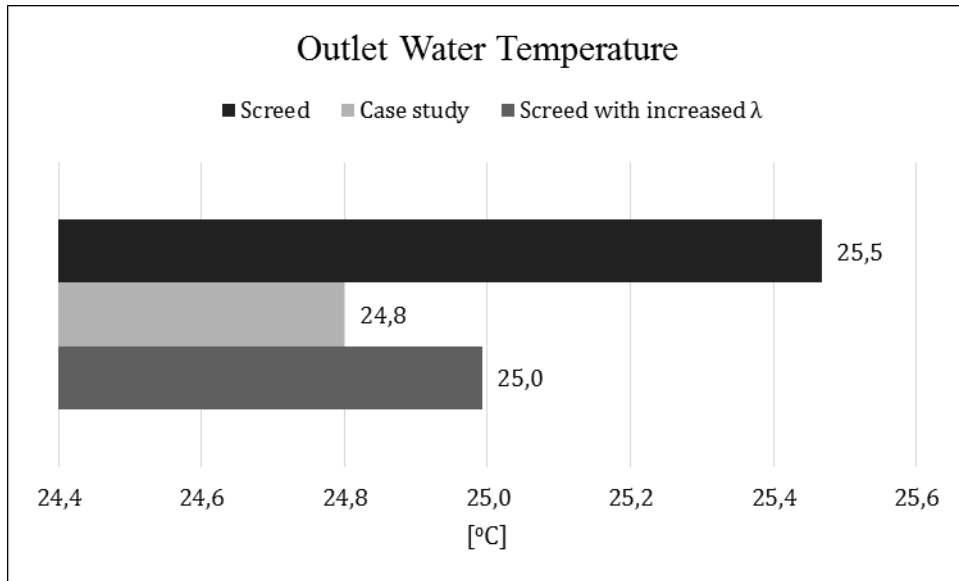*Figure 6.9 Surface temperature of increased thermal mass in floor construction*

Figure 6.10 Outlet water temperature with increased thermal mass of floor construction

6.2.3 Transient analysis with improved thermal mass

When simulating the improved thermal mass transient, it is noticed that it takes longer time for the improved solution to adapt to disturbances, see Figure 6.11. It has nearly not even evened out before the other disturbance happens. When the disturbance stops it is also seen that it takes about a day more before the upward heat transfer is steady. As for the stationary analysis, the screed solution with increased λ results in a higher upward heat transfer rate than using Portland cement.
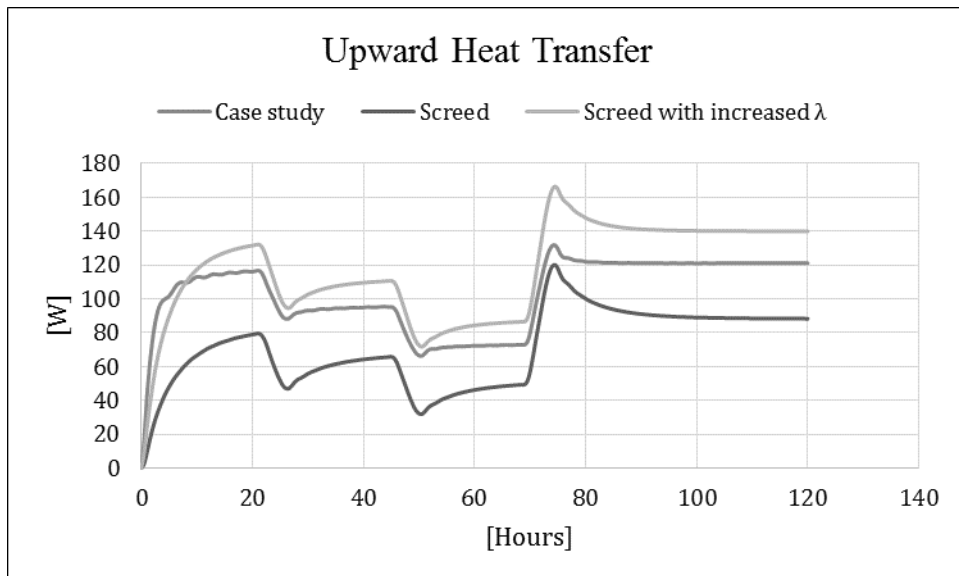

Figure 6.11 Upward heat transfer when simulating transient with increased thermal mass in floor construction

When comparing the outlet water temperature, the outlet water temperature is higher as for the stationary simulations, see Figure 6.12. The adjustment to the

disturbances also takes longer time, and the outlet temperature does not have any fast temperature drops in comparison with the case study. Further, the outlet water temperature of the screed solution also contains hourly variations, which occurs at the increase/decrease of a disturbance. When using the screed with increased λ, the outlet water temperature is lowered compared to the Portland cement. In comparison with the case study results, both of them have higher outlet water temperature, as in the stationary analysis, hence more heat can be removed from the heated water.
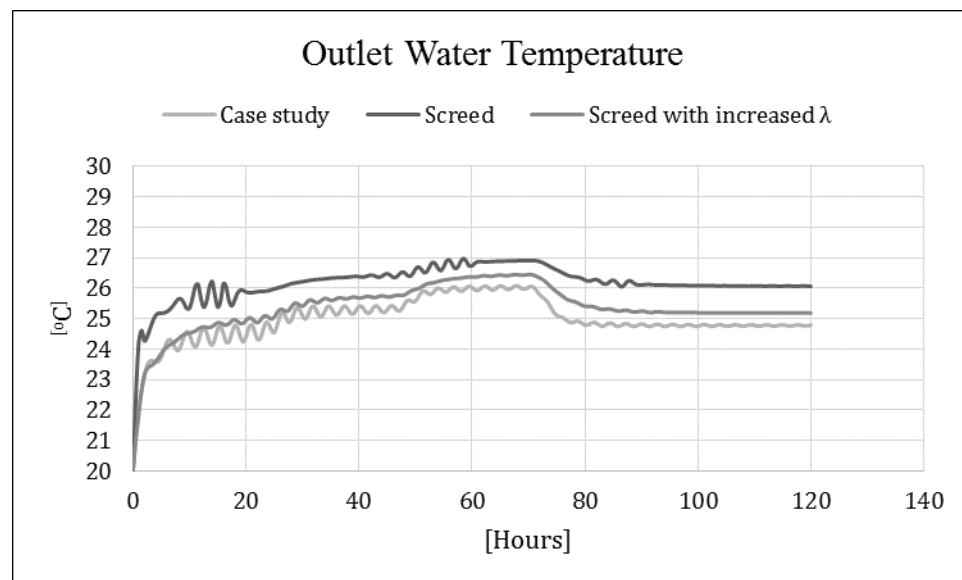

Figure 6.12 Outlet water temperature when simulating transient with increased thermal mass in floor construction

In future analysis, only the Portland cement solution is investigated further.

6.3   Improvement of thermal mass in apartment unit

The third improvement is to increase the thermal mass in the apartment unit, to obtain similar performance of the floor heating system as embedded into a heavy-weight floor construction. The investigation consists of adding gypsum boards with phase change material inside the apartment unit, where heat can be stored and used when needed.

Phase change materials, PCMs, is materials with a latent heat storage capacity (Sharma et al, 2007). The heat storage capacity occurs when the material changes phase, from solid to liquid or reverse, at different temperatures (Sharma et al, 2009). A typical example is when water transfers from liquid phase to gas phase when boiling. To make the water boil extra heat is added, thereby heat is stored inside the material.

When modelling phase change material, the specific heat capacity as well as thermal conductivity is varying depending on the temperature. With the added PCM, the number of changeable variables increases which requires more computer capacity than available. A suggestion is to simplify the model further, but then the ability to compare results will be affected. Thereby was the

improvement of increasing thermal mass inside the apartment unit not successfully investigated.

6.4 Combination of improved heat distribution and thermal mass

From previous evaluation, the screed solution with Portland cement requires better heat distribution and the graphite grid did not give big difference due to less thermal conductivity in z-direction. By combining these improvements, the screed solution might increase its ability to transfer heat, with still obtaining its performance similar to a heavy-weight floor.

The graphite grid is placed as previous improvement, close to the pipe, but embedded into the screed. As for the improvement with graphite grid, also an alternative with increased interface is investigated.

6.4.1 Stationary analysis improved heat distribution and thermal mass

When combining the improvement of heat distribution and thermal mass, an improvement of upward heat transfer is obtained compared with improving them separately. Furthermore, the difference between the two interfaces of graphite grid is decreased while embedded into screed. This might be because the screed has better possibilities to take advantage of the low thermal conductivity in z-direction. As for the graphite grid solution, the downward heat transfer is lower for the improvement compared with the case study, but with a minor difference. The floor surface temperature of the investigations follows the heat transfer division.
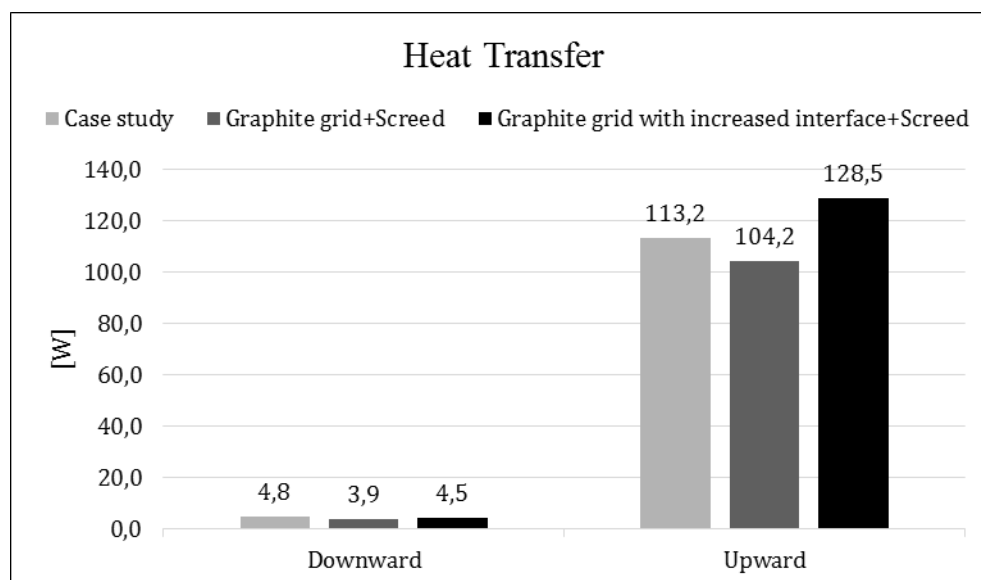

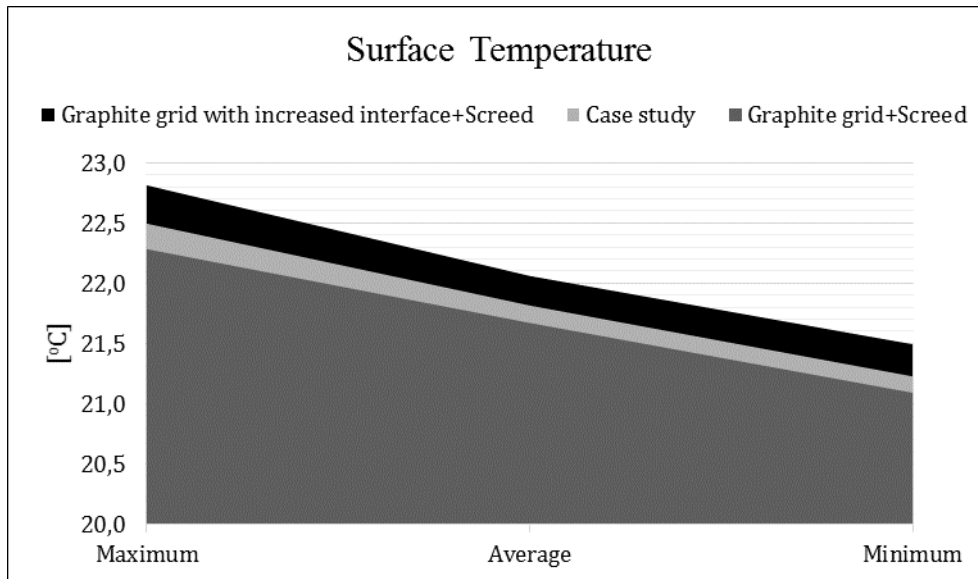*Figure 6.13 Upward and downward heat transfer or combined solution*

Figure 6.14 Surface temperature of combined solution

An interesting result is outlet water temperature, which is the same for the case study analysis and combined improvement with increased interface. But as mentioned above the heat transfer is higher of the combined solution with increased interface. This indicates by increasing the thermal inertia, a better upward heat transfer is generated.
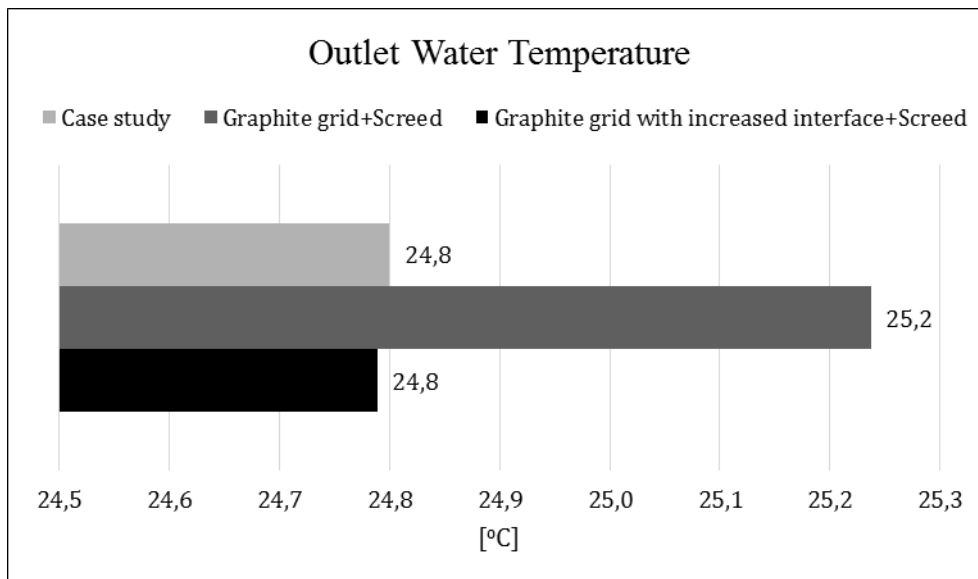

Figure 6.15 Outlet water temperature of combined solution

As for improvement one, the solution with increased interface is more interesting to investigate further.

6.4.2 Transient analysis with improved heat distribution and thermal mass

When studying the combined improvement transient is it seen that the upward heat transfer is increased, and it is only in the beginning and end of the

disturbance that an increased time constant is noticed, see Figure 6.15. This indicates that the thermal inertia is affecting the solution. This is also seen when comparing the outlet water temperature, where it is more stable and even than the case study model, see Figure 6.16.
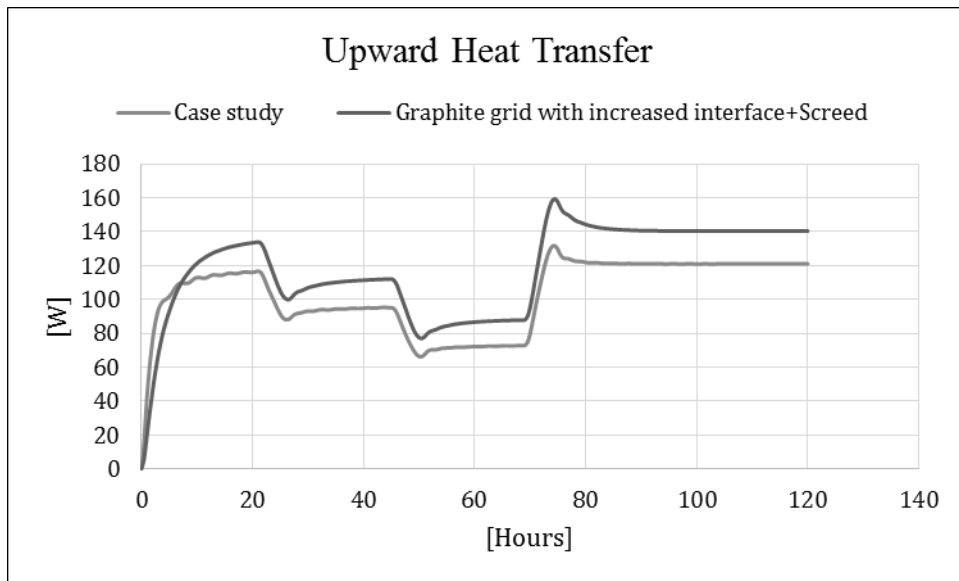

Figure 6.16 Upward heat transfer when simulating transient with combined solution
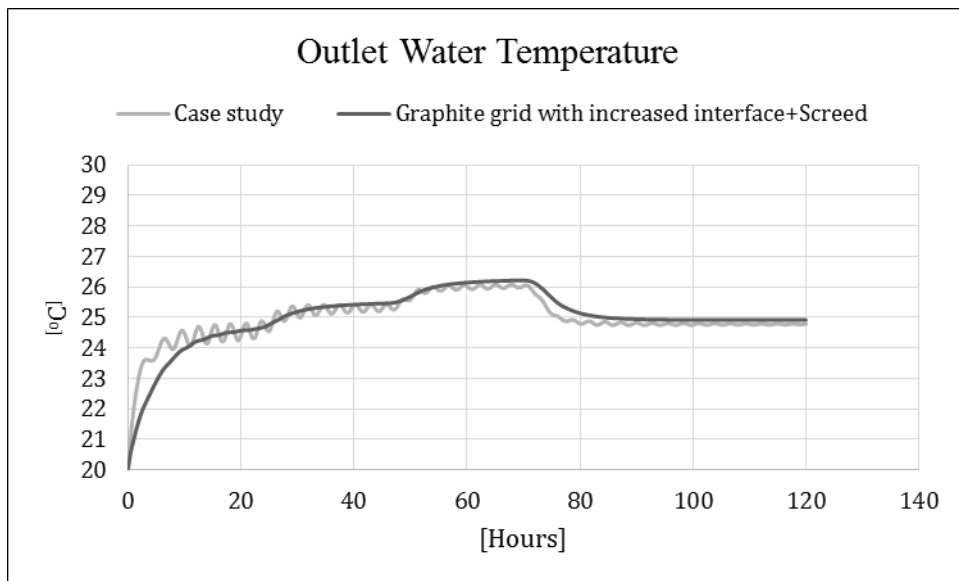

Figure 6.17 Outlet water temperature when simulating transient with combined solution

7   Conclusion

In this study, in-depth numerical models of a floor heating system have been developed with the aim to investigate potential improvements of floor heating systems embedded into light-weight floor constructions of HSB Living Lab.

The COMSOL Multiphysics modules Heat Transfer in Solids and Heat Transfer in Pipes, were chosen as method of the in-depth numerical model. The verification of the reference model, presented a more detailed in-depth numerical model than expected due to differences comparing with the semi-analytical calculation method. The differences revealed an ununiformed temperature distribution of the pipe cross section, instead of a constant temperature distribution assumed by the calculation method. Furthermore, the Heat Transfer in Pipes module included corrections due to viscous heat and friction, which probably explained the ununiformed temperature distribution.

By the transient analysis of the case study model, the floor heating system embedded into a light-weight floor construction showed ability to self-regulate. Further, the study presented a regulation with fast correction time and nearly direct adjustments to disturbances. The transient analysis showed a decreased upward heat transfer when simulating with an exponential indoor temperature, due to less difference between floor surface temperature and indoor temperature. When a positive disturbance occurs indoors the indoor temperature increases, thereby the in-depth numerical model with exponential indoor temperature corresponded to reliable results.

Three theoretical ideas of improvements were investigated to increase the performance of the floor heating system embedded into HSB Living Lab. The first improvement was increased heat distribution of the floor construction, the second improvement was increased thermal mass of the floor construction and the third improvement was increased thermal mass of the apartment unit. From the analysis, improvement two and a combination of improvement one and two had improved performance of the floor heating system.

The improvement with increased heat distribution of the floor heating system should by theory transfer additional heat upwards, due to a developed ability to take advantage of heat inserted into the floor construction. The investigation consisted of replacing previous heat distribution plates with a heat distribution grid of graphite. Compared with aluminum, graphite has a higher heat conductance in x- and y-direction but a lower heat conduction in z-direction. The investigation resulted in an unaffected upward heat transfer, due to decreased heat conduction in z-direction. Furthermore, the decreased difference between maximum and minimum floor surface temperature was a result of the increased heat conduction in x- and y-direction. When the interface between the pipe and grid was increased, the insulation efficiency of the floor construction improved. Thereby, the conclusion of the investigated improvement is importance of a high heat conduction in z-direction as well as the interface between pipe and heat conductive layer.

There two potential improvements investigated when increasing the thermal mass, should by theory function similar as a floor heating system embedded into a heavy-weight floor construction. Thereby, slowly adjust to disturbances indoors and obtain an ability to store heat.

The first potential improvement with increasing thermal mass was to obtain heat storage capacity of the floor construction by increased thermal mass of the floor construction. The investigation consisted of remaining the floor construction similar as previous, but improve the upper part by embed the water pipes into screed. When using a screed with Portland cement properties, the study resulted in an increased difference in floor surface temperature causing a decreased upward heat transfer. Due to a decreased water temperature difference, additional heat could be extracted from the heated medium. When using a screed with high thermal conductivity, the upward heat transfer had a significant improvement. The difference in water temperature was decreased and compared to the screed with Portland cement properties more heat was extracted from the heated water. Thereby, it is important to embed the pipes into a screed with high thermal conductivity to obtain a performance improvement and take advantage of the heat inserted into the floor heating system. The transient study with screed solution presented an increased adjustment time to disturbances, which indicated a similar function as a heavy-weight floor construction.

To improve the upward heat transfer of the investigation with Portland cement, a combination with graphite grid was studied. By theory, the combined alternative should improve the heat distribution and obtain a similar performance as a heavy-weight floor construction. The study resulted in an increased upward heat transfer as well as a decreased water temperature difference. Thereby, the combined solution has a performance improvement of the floor heating system. The transient study of the combined solution presented a time delay to disturbances and acted similar as a floor heating system embedded into a heavy-weight floor construction.

The second potential improvement with thermal mass was to increase the thermal mass in the apartment unit. In other words, the heat storage capacity was in the apartment unit while the floor construction continued performing as a light-weight floor. The investigation consisted of using phase change materials, which stores and releases heat when depending on positive or negative heat disturbance. Due to lack of computer capacity when simulating the models, the investigation was not succeeded. Therefore, the improvement with phase change materials is interesting to investigate in the future.

8 Further investigations

Future interesting investigations regarding potential improvements of floor heating systems are to investigate other heat distribution materials and the influence of phase change material in the apartment unit, as mentioned in Chapter 7. Regarding the heat distribution material, a material with higher thermal conductivity in z-direction would be preferable. As well as the differences between theoretical investigations with changed heat distribution material and experimental investigations.

Concerning the in-depth numerical model, some investigations can develop it. To decrease the prescribed parameters, simulating the air box with CFD-simulations can be further investigated. Studies of the transient analysis can present how the indoor temperature increases or decreases due to disturbances as well as find when the system shuts off.

The chosen method, with Heat Transfer in Pipes module, presented an unexpected detailed level of the in-depth numerical model due to the temperature distribution in the pipe cross section. Further investigation regarding the temperature distribution as well as the temperature distribution in the semi-analytical method might provide additional knowledge about the analyzed differences.

9 References

Balaÿ, P., Hagy, S. (2014) *Adaptable Design for the HSB Living Lab: flexible, co-created spaces in student housing*. Gothenburg: Chalmers University of Technology. (Master Thesis in the Master's Programme Design for Sustainable Development).

Boverket. (2015) BFS 2015:3 - BBR 22. *Boverket*. http://www.boverket.se/sv/lag--ratt/forfattningssamling/gallande/bbr---bfs-20116/. (Accessed 2016-04-18).

Boverket et al. (2002) *Grundtips för golvvärme*. Stockholm: EQ Print.

COMSOL. (2016) COMSOL Multiphysics. *COMSOL*. https://www.comsol.se/comsol-multiphysics. (Accessed 2016-04-13).

COMSOL. (2015) *Pipe Flow Module User's Guide*.

Engineering Toolbox. (2016) *Gases – Ratios of Specific Heats*. http://www.engineeringtoolbox.com/specific-heat-ratio-d_608.html. (Accessed 2016-05-22)

Hagentoft, C.-E. (2001) *Introduction to Building Physics*. Lund: Studentlitteratur.

Hagentoft, C-E., Karlsson, H. (2011) Byggnadsintegrerad uppvärmning. *SBUF*. http://vpp.sbuf.se/Public/Documents/ProjectDocuments/2daab022-b576-4e7e-9fa7-9da94da8f728/FinalReport/SBUF%2011991%20Slutrapport%20Golvv%C3%A4rme%20M%C3%B6jligheter%20med%20byggnadsintegrerad%20uppv%C3%A4rmning.pdf. (Accessed 2016-05-10)

Holladay, M. (2013) All about thermal mass. *Green Building Advisor*. http://www.greenbuildingadvisor.com/blogs/dept/musings/all-about-thermal-mass. (Accessed 2016-02-28).

HSB Living Lab. (2016) What's HSB Living Lab. *HSB Living Lab*. https://www.hsb.se/kampanjer/hsblivinglab/Om/. (Accessed 2016-04-18).

HSB Living Lab. (2016) Stay here. *HSB Living Lab.* https://www.hsb.se/kampanjer/hsblivinglab/stayhere/. (Accessed 2016-04-18).

Karlsson, H. (2008) Self-Regulating Floor heating systems in low energy buildings. *ResearchGate*. https://www.researchgate.net/publication/282076099_Self-Regulating_Floor_Heating_Systems_in_Low_Energy_Buildings. (Accessed 2016-05-10)

Karlsson, H. (2010) *Thermal modelling of water-based floor heating systems: Sypply temperature optimization and self-regulation effects*. Gothenburg: Chalmers University of Technology. (Thesis for the degree of doctor of philosophy in Department of Civil and Environmental Engineering).

Morini, G. L., (2013) Viscous Heating. In *Encyclopedia of Microfluidies and Nanofluidies*. http://link.springer.com/referencework/10.1007/978-3-642-27758-0/page/v/1. (Accessed 2016-05-25)

Rennie, R. (2016) A Dictionary of Chemistry (7 ed.). *Oxford Reference*. http://www.oxfordreference.com/view/10.1093/acref/9780198722823.001.0001/acref-9780198722823-e-739#. (Accessed 2016-05-20)

Pierson, H O. (1993) *Handbook of Carbon, Graphite, Diamonds and Fullerenes*. [Elektronisk]. New Jersey: Noyes Publications.

Sharma, A., Tyagi, V.V., Chen, C.R., Buddhi, D. (2007) Review on thermal energy storage with phase change materials and applications. *Renewable and Sustainable Energy Reviews*. October 9th. http://www.sciencedirect.com/science/article/pii/S1364032107001402. (Accessed 2016-06-20)

Appendices

Appendix A – Description of wall construction of the Standard room

External wall construction

The external wall construction consists of wooden studs, cc600, with mineral wool insulation, see Figure A.1. A standard window, with the recommended U-value of 1.2 W/m² according to Boverket (2015), is placed into the external wall. The window area covers 50 % of the external wall area.

The recommended U-value according to Boverket (2015) of a wall construction is 0.18 W/m². To fulfil the recommendation the stud and insulation needs to be 170 mm thick.

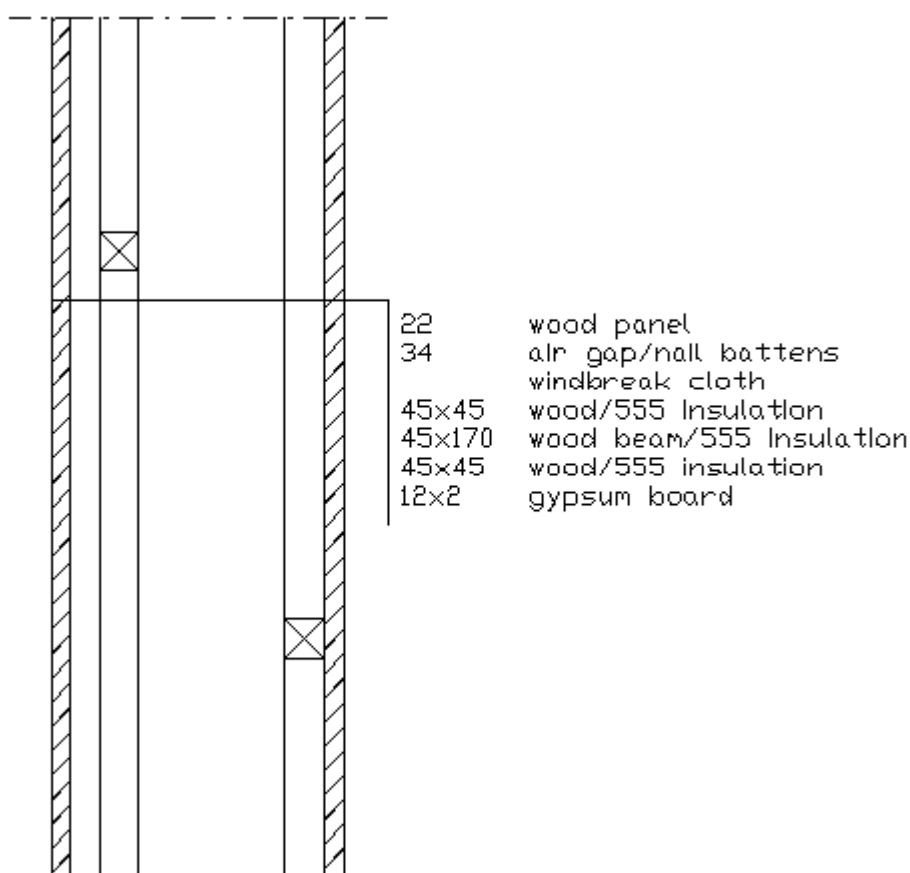|	
22	wood panel
34	air gap/nail battens
	windbreak cloth
45×45	wood/555 insulation
45×170	wood beam/555 insulation
45×45	wood/555 insulation
12×2	gypsum board

Figure A.1 Geometry and materials of external wall in standard room

Internal wall construction

The internal wall construction consist of wooden studs, cc600, with mineral wool insulation in between due to acoustic requirements, see Figure A.2. Because the insulation only takes acoustics into account, the U-value is not of interest. Therefore no adjustment is made which results in a U-value of 0.4 W/m².
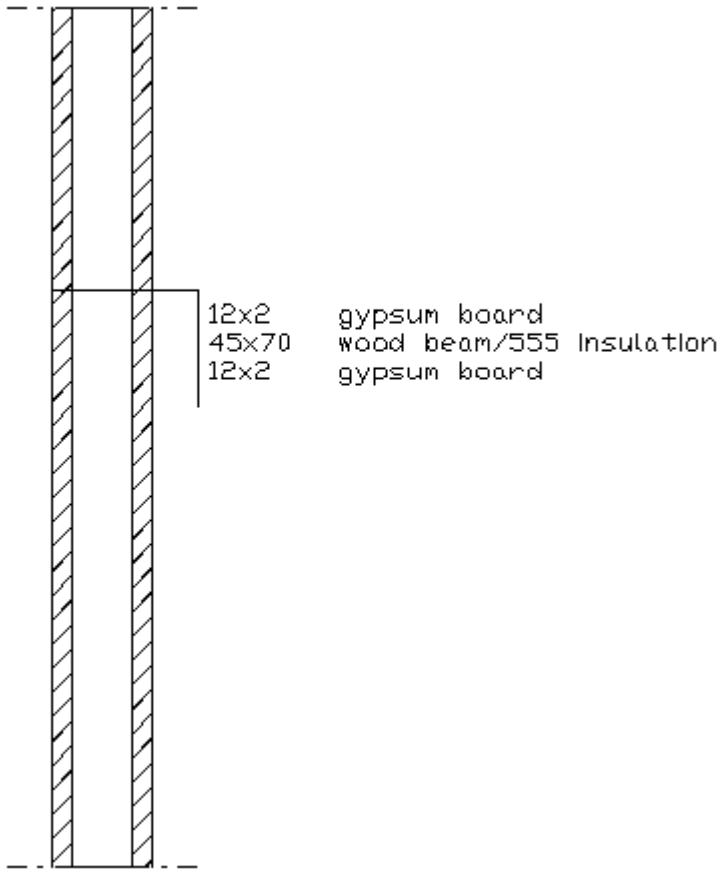
Figure A.2 Geometry and material of internal wall in standard room

Appendix B – Standard room calculations
Heat demand calculations
The heat demand is calculated by equation (2.10) mentioned in Section 2.3, see
Table B.1.

Table B.0.1 Input data and calculation result of heat demand calculations

Parameter	Value	Unit
$T_{exterior}$	-16	^{o}C
$T_{interior}$	22	^{o}C
U_{wall}	0.178	W/m^2K
U_{window}	1.2	W/m^2K
A_{wall}	4.433	m^2
A_{window}	4.433	m^2
Q_{demand}	232	W
q_{demand}	25.04	W/m^2

Calculation method
With the method described in Section 3.2, heat flux and insulation efficiency of
the floor construction in standard room is calculated. The heat fluxes is
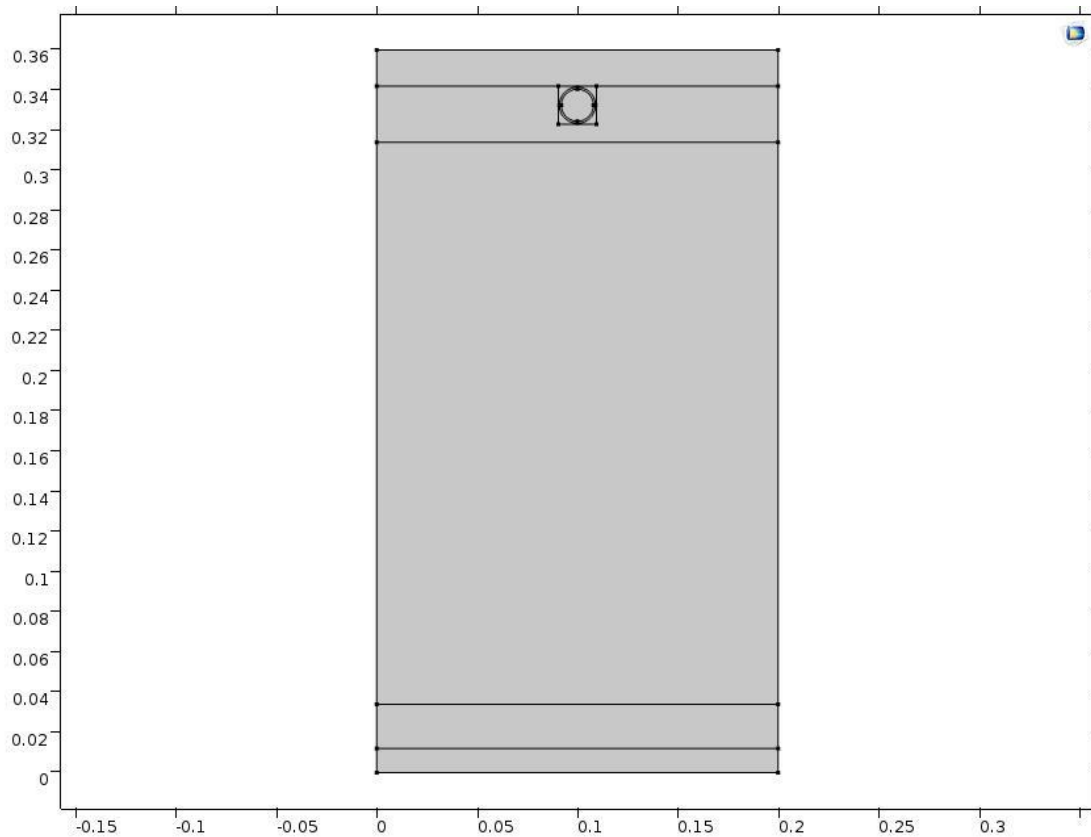calculated by creating a 2D numerical model in COMSOL Multiphysics, see Figure
B.1.

Figure B.1 2D model of the cc-distance of the pipes in the standard room

Due to different cross sections with stud and insulation, heat flux of both structures is simulated and then calculated by the proportion. With the inlet water fluid of 1 ºC and the indoor temperature of 0 ºC, simulation results of the upward and downward heat flux is obtained, see Table B.2

Table B.2 Calculation results of standard room

Parameter	Value	Unit
$\gamma_{up,stud}$	0.656	W/mK
$\gamma_{down,stud}$	0.069	W/mK
$\gamma_{up,insulation}$	0.662	W/mK
$\gamma_{down,insulation}$	0.023	W/mK
t_{stud}	0.045	m
cc_{stud}	0.600	m
Percentage stud	0.075	-
Percentage insulation	0.925	-
γ_{up}	0.661	W/mK
γ_{down}	0.026	W/mK
η	0.962	-

Appendix C – Comparison of simplified transient model

To decrease simulation time while simulating transient studies, a simplified transient model is created. The thermal conductivity of the material is adjusted to obtain similar results as for the stationary case. When simulating the transient model with a thermal conductivity of $\lambda = 0.06$ W/mK, the difference between the stationary model and simplified transient model is insignificant, see Table D.1. Furthermore, a decrease of 2 minutes in simulation time is obtained.

Table D.1 Comparison between stationary model and simplified transient model with a thermal conductivity of λ=0.6 W/mK

Parameter	Stationary model	Simplified transient model	Difference
Q_{down}	4.8 W	4.3 W	0.5 W
Q_{up}	113.2 W	113.3 W	0.1 W
$T_{surf,max}$	22.5 ᵒC	22.5 ᵒC	0 ᵒC
$T_{surf,average}$	21.8 ᵒC	21.8 ᵒC	0 ᵒC
$T_{surf,min}$	21.2 ᵒC	21.2 ᵒC	0 ᵒC
T_{outlet}	24.8 ᵒC	24.8 ᵒC	0 ᵒC
T_{inlet}	28.0 ᵒC	28.0 ᵒC	0 ᵒC